Received: 15 February 2021 | Revised: 23 December 2021 | Accepted: 30 December 2021

DOI: 10.1002/esp.5322

RESEARCH ARTICLE

ESPL WILEY

How strong are salt marshes? Geotechnical properties of coastal wetland soils

Helen Brooks[1,2] | Iris Moeller[2] | Tom Spencer[1] | Katherine Royse[3] | Simon Price[4] | Matt Kirkham[3]

[1]Department of Geography, University of Cambridge, Cambridge, UK

[2]Department of Geography, Trinity College Dublin, Dublin 2, Ireland

[3]British Geological Survey, Nottingham, UK

[4]Arup, London, UK

Correspondence
Helen Brooks, Department of Geography, Trinity College Dublin, Museum Building, Dublin 2, Ireland.
Email: helen.brooks@newcastle.ac.uk

Funding information
British Geological Survey; Natural Environment Research Council, Grant/Award Numbers: NE/L002507/1, NE/N015878/1, NE/R01082X/1

Abstract

Salt marshes are globally distributed, vegetated intertidal wetlands and marsh edge erosion is common on many shores. To understand how and why marsh edge erosion occurs, the response of salt marsh substrates to applied shear and vertical stress must first be quantified. This response is likely influenced by marsh substrate biological, geochemical and sedimentological composition. However, currently there is little systematic research into the between-marsh variability in these properties and how they affect both marsh edge erosion processes and the ability of a marsh to maintain its position vertically within the tidal frame.

This paper compares two marshes of contrasting sedimentology at Tillingham marsh, East England and Warton marsh, Northwest England. Soil shear strength and compressibility are determined by applying geotechnical methods to determine marsh resistance to shear and vertical effective stresses. This research was able to isolate the influence of roots on substrate shear strength in a three-dimensional sample. In response to vertical effective stress, both the expected displacement magnitude and the vertical recovery potential of a marsh substrate are affected by past stress conditions on the marsh, particularly those resulting from desiccation. The substrate response to vertical effective stress also influences substrate shear strength through the effect of consolidation on the void ratio (or bulk density).

We present evidence for the connection between marsh composition and substrate behaviour under applied stress. The results shed light on potential determinants of marsh resistance to edge erosion, which is ultimately essential for the informed implementation of both nature-based coastal flood defences and coastal restoration schemes.

KEYWORDS
Dengie Peninsula, Morecambe Bay, nature-based solutions, oedometer, ring shear, saltmarsh, shear box, tidal wetlands

1 | INTRODUCTION

Salt marshes (vegetated intertidal platforms) provide important regulating, provisioning and cultural ecosystem services (Foster et al., 2013; Spalding et al., 2014). One particular service is that of hazard regulation, whereby marsh surfaces are efficient storm surge, current and wave dissipaters during infrequent high-energy events (Möller et al., 2014). It has therefore been argued that the presence of such wetlands often lowers the risk of flooding and reduces erosion and maintenance costs of landward-lying flood protection structures (Beaumont et al., 2008).

However, salt marsh area loss has been recorded on many coastlines worldwide (Blankespoor et al., 2014; e.g. Northwest Europe: Baily & Pearson, 2007; van der Wal & Pye, 2004). Future marsh areal

loss is also of concern, both from ongoing and near-future accelerated sea-level rise where landward marsh migration is not possible (Schuerch et al., 2018), and changes in temperatures and precipitation patterns which can adversely affect the marsh vegetation (Strain et al., 2017). This widespread area loss and concern over external pressures has raised important questions regarding the future persistence of salt marshes and the ecosystem services they support.

In European salt marshes, marsh platform elevation, tidal inundation and sedimentation are strongly linked, through a form–process feedback (French, 2006). Understanding changes in the vertical stability of the marsh platform is therefore critical. One component of this is the ability of the marsh substrate to withstand vertical stress. For marsh platforms exposed to loading from exceptional water depths during storm events on the Gulf and East Coasts of the United States, Cahoon (2003) observed a range of field responses to storm surge inundation, from surface compression and near-complete rebound, to an overall increase or decrease in elevation. However, how this range of responses can be generated remains poorly understood.

Whilst much recent saltmarsh research has looked at marsh response to sea-level rise and, as a consequence, has had a strong focus on vertical performance and stability, the loss of saltmarsh area has drawn attention to the need to know more about lateral stability. Empirical studies suggest that the rate of marsh edge erosion may correlate with wave power (e.g. Leonardi et al., 2016), but models used to simulate marsh edge erosion assume a spatially homogeneous substrate (vertically and horizontally) and thus far do not incorporate different substrate properties. Understanding marsh edge erosion processes and marsh stability first requires an understanding of how the substrates behave when subjected to an applied force. Marsh edge erosion processes include (a) cliff undercutting followed by cantilever failure or gravitational slumping once the overlying section weight exceeds the substrate strength (e.g. Allen, 1989, 2000; Bendoni et al., 2014; Francalanci et al., 2013) and/or (b) tension crack formation during substrate drying and subsequent toppling failure (e.g. Bendoni et al., 2014; Cola et al., 2008; Francalanci et al., 2013). While there is a general consensus among existing studies that such processes contribute to marsh edge erosion, observations of such erosion are rare and difficult to capture (e.g. Godfrey et al., 2020). As such, the erosion processes causing retreat are generally inferred from marsh morphology change after erosion has taken place and are therefore poorly understood.

What is less well understood is precisely *how* marsh edge erosion occurs: firstly how biophysical processes achieve marsh substrate removal and secondly how the geotechnical and sedimentary properties that may relate to spatial variations in substrate resistance to erosion vary *within* and *between* marshes of different substrate composition. This paper deals with the latter.

We use a laboratory study because the specific substrate properties controlling the mechanics of vertical and horizontal substrate deformation or failure are best tested on substrates in the laboratory, free from the confounding influences that accompany the observation of storm surges and tidal inundations in the field.

Here, 'marsh stability' describes the ability of marsh surface and margin substrates to resist the shear and vertical stress applied by gravity, waves, tides, storm surges, overburden and water table changes over timescales of hours or more. In a vertical direction, we distinguish between total stress (applied stress) and effective stress (total stress minus pore water pressure). In this paper, substrate shear strength relates particularly to the bulk resistance of the marsh substrate to shear stress. Shear strength can be divided into a cohesional component (resulting from, amongst others, electrostatic forces between particles, root cohesion and apparent cohesion from suction; Barnes, 2010) and a frictional component (resulting from interparticle contacts; Knappett & Craig, 2012). Frictional strength is only important when the substrate is subjected to vertical or, in some cases, horizontal stress, and when that stress causes particle interlocking. Shear strength is distinct from erodibility, although the difference between the two terms is poorly defined in the literature (see Brooks, 2020). Erodibility relates to the critical erosion shear stress (the substrate resistance to grain-by-grain erosion), and this is not measured in this study. Given that substrate composition (e.g. particle size, root content and organic content) will affect cohesion (Zhang & Hartge, 1990) and the degree of particle interlocking (friction; Alias et al., 2014; Kara et al., 2013), this paper aims to understand the influence of substrate composition on bulk substrate shear strength in a laboratory setting. There comes a point where substrates are subject to shear stress which exceeds the frictional and cohesional strength of that substrate and erosion follows. It is important to understand how substrate composition affects frictional, cohesional and ultimately shear strength to explain how marshes erode and therefore how salt marsh stability may change in the future.

This paper applies a range of geotechnical tests to two sedimentologically contrasting salt marsh substrates, with the aim of better constraining the range of salt marsh substrate properties that control marsh substrate strength and deformation and showing how, within this range, variations in geotechnical properties link to substrate composition. Fundamentally, the application of such methods offers an opportunity to better understand how a marsh substrate behaves under stress application from waves, currents or water level changes (e.g. Callaghan et al., 2010; Tonelli et al., 2010) in a closely controlled environment which cannot be achieved using a shear vane or cohesive strength meter (e.g. see Watts et al., 2003).

Shear box and ring shear tests are able to determine peak and residual substrate shear strengths, respectively, in response to longer-term changes in the sediment overburden or water table (two influential factors on the stress environment which have hitherto been rarely considered in salt marsh studies). These tests also quantify the cohesional strength and the effective angle of shearing resistance (Table 1), which can be linked to salt marsh substrate composition. While ring shear tests generally consider the response of a previously failed substrate to large shear stresses, the roots were removed for these tests in this study, allowing us to assess the influence of roots on substrate strength. Oedometer tests determine the magnitude of vertical deformation caused by a vertical effective stress and whether such deformation is either permanent or recoverable (Table 1). Vertical deformation is tightly linked to the shear strength of a substrate through the influence of bulk density on substrate shear strength, and this shear strength can be measured using a shear box test. This type of deformation therefore must be understood in order to determine how substrate shear strength might change over time as substrate consolidation changes. There has been little previous application of laboratory-based geotechnical methods to salt marsh substrates, with the main purpose of better understanding the substrate behavioural properties. Where such techniques have been applied, the focus has

TABLE 1 Table summarizing what the methods measure and how this is relevant to marsh substrate stability/strength

Method	Property measured	Link between measured property and marsh substrate stability/strength (see definitions in Introduction)
Particle size analysis	Particle size of sediment sample, reflected in the median grain size (D_{50})	Finer, cohesive sediments (with a lower D_{50}) generally exhibit greater strength in shear (e.g. Ford et al., 2016; Lo et al., 2017).
	Uniformity coefficient (U_c, defining the range of grain sizes)	A high U_c (>4) indicates that there is a wide range of particle sizes within the sample. This usually allows a greater packing density, which is then reflected in a higher bulk density, lower void ratio and therefore more interparticle contacts.
Oven drying	Root mass content	Roots provide tensile strength and can increase substrate strength (e.g. Chen et al., 2012; Ford et al., 2016; Lo et al., 2017; Wang et al., 2017).
Shear box	Peak substrate shear strength for a given vertical effective stress (τ_f)	A higher peak shear strength indicates that the substrate can resist a higher applied shear stress.
	Effective cohesion (c')	This reflects the soil shear strength when exposed to neither vertical stress nor confining pressure (Head, 1981) and reflects the electrostatic forces between particles.
	Effective angle of shearing resistance (φ')	The component of soil shear strength provided by interparticle friction (Head, 1981). This increases as interparticle contacts increase.
Ring shear	Residual shear strength for a given vertical effective stress (τ_f). This reflects the strength retained after failure.	Substrates can often withstand a lower stress (indicated by residual strength) if they have failed previously. Usually, strength reduction occurs as clay platelets reorientate to border the failure plane. As roots were removed for these tests (in line with BS1377, and unlike for the shear box tests), this reduction in strength compared to the peak shear strength was hypothesized to also reflect the loss of roots.
	Residual effective angle of shearing resistance (φ_r')	As above, this usually reflects the component of soil shear strength provided by interparticle friction. As roots were removed for ring shear tests in this study (see above), any reduction in the residual effective angle of shearing resistance may also reflect the loss of roots.
Oedometer	Axial (vertical) displacement in response to a vertically applied effective stress.	Indicates the vertical displacement (and therefore change in surface elevation) in response to a vertically applied effective stress. If this is irrecoverable (see OCR below), this has implications for marsh platform inundation frequency and sediment supply.
	Change in void ratio (a proxy for bulk density) in response to this vertically applied effective stress	Increased bulk density is known to increase substrate shear strength (Watts et al., 2003).
	Pre-consolidation pressure (maximum previous vertical effective stress to which the soil has been subjected)	In the case of salt marshes this most likely reflects the influence of desiccation on pore water pressures.
	Overconsolidation ratio (OCR)	Tells us about the magnitude of vertical displacement, and the substrate vertical recovery potential, following unloading. When OCR < 1, the sample is normally consolidated so has not previously been exposed to a vertical effective stress greater than that it was exposed to immediately prior to sampling. A sample is overconsolidated when OCR > 1, so the sample has previously been exposed to a higher vertical effective stress than that immediately prior to sampling. If OCR < 1, large, irrecoverable vertical displacement is expected. If OCR > 1, small, recoverable vertical displacement can be expected, until a stress is applied which exceeds the pre-consolidation pressure.

not been on understanding marsh substrate response to applied stress. Rather, previous studies have been applied to 'decompact' vertical marsh sequences for the purpose of improving sea-level reconstructions from marsh cores (Brain et al., 2011, 2015, 2017). By improving understanding of the links between marsh substrate composition and behaviour, this paper does not intend to mimic real-world processes, but does provide a first step towards improving the understanding of salt marsh stability. This paper characterizes the intrinsic soil geotechnical properties, then considers how these properties might affect the response of the substrate to applied stress in natural settings.

2 | FIELD SITES

This study focuses on two UK open coast marshes with minerogenic content >85%, as is characteristic of Northwest European marshes (Allen, 2000). However, the two marshes have contrasting clay, silt and sand contents.

2.1 | Tillingham marsh

Tillingham marsh is located on the central section of the Dengie Peninsula, Essex, UK (Figure 1) and reaches 800 m wide. The marsh–mudflat transition is characterized by a well-developed, shore-normal ridge–runnel morphology (Schuerch et al., 2019), with mudflats stretching approximately 4 km offshore. Over the past 100–150 years, the Dengie marshes have demonstrated dynamic behaviour, with evidence of both advancing and retreating phases (Harmsworth & Long, 1986; Pye & French, 1993; van der Wal & Pye, 2004).

Tillingham marsh sediments are clay/silt-dominated (Ford et al., 2016). The near-horizontal vegetated platform lies at an elevation of 1.9–2.7 m ODN (Ordnance Datum Newlyn, where 0.0 m ODN approximates mean sea level) and is inundated approximately 10% of the time (unpublished data, Cambridge Coastal Research Unit). The mid/upper marsh (2.4–2.7 m ODN) is colonized by *Puccinellia maritima*, *Limonium vulgare* and *Atriplex portulacoides* (Möller, 2006). Low marsh and pioneer communities occur at elevations ≤2.4 m ODN (Rupprecht et al., 2015), with patches of *Spartina anglica*, *Salicornia* spp., *Suaeda maritima* and *Aster tripolium*. The marsh is ungrazed.

The Mean Spring Tide Range is 3.7 m at Harwich, 30 km northeast of Tillingham marsh. At the vegetated marsh edge, Möller and Spencer (2002) recorded water depths of 0.12–0.84 m and mean and maximum significant wave heights of 0.26 and 0.86 m, respectively, between September 2000 and July 2001. Exceptionally high water levels have been observed when storm surges coincide with high-tide levels. For example, during the 8 January 2019 storm surge, the water depth above the marsh surface adjacent to the sea wall reached

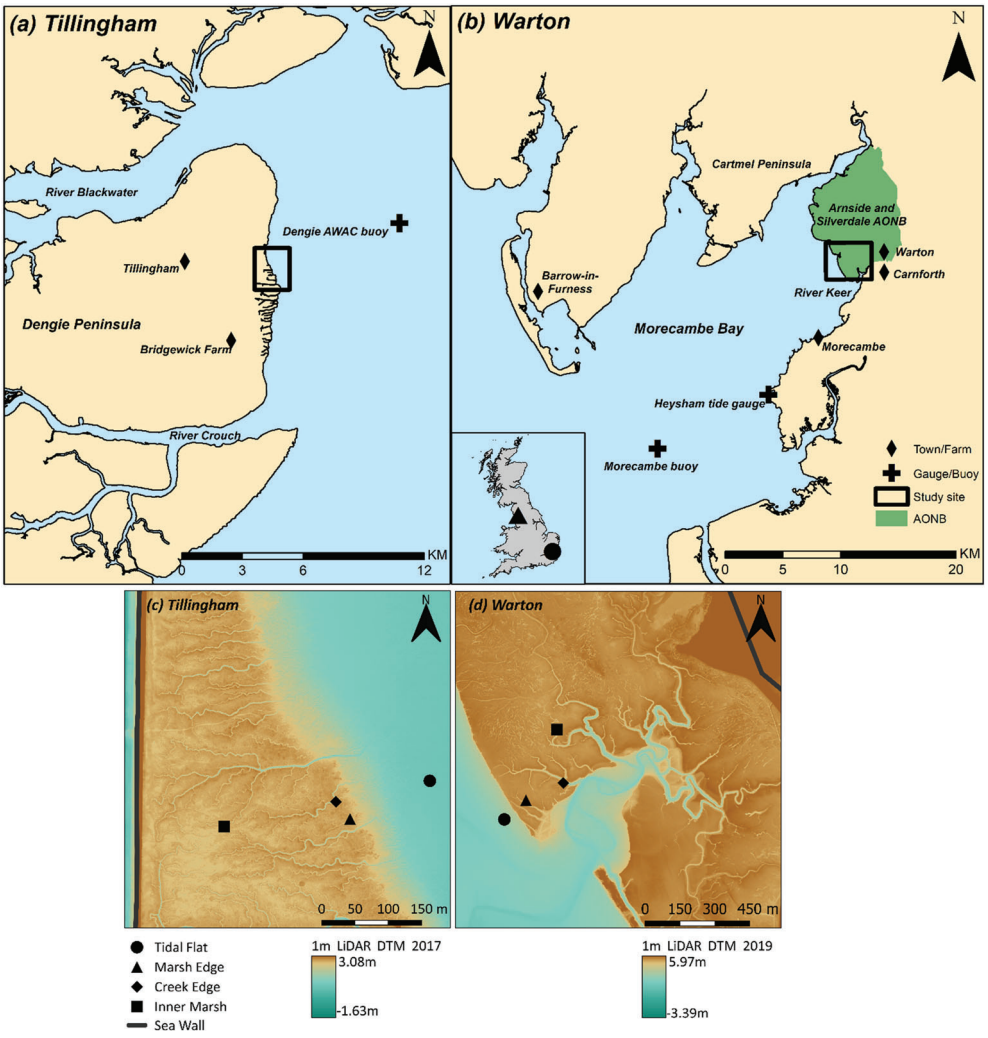

FIGURE 1 Site map of Tillingham marsh (a, c) and Warton marsh (b, d). The Arnside and Silverdale area of outstanding natural beauty (AONB) is shown in green. In the UK map inset, the circle represents Tillingham, while the triangle represents Warton. For the basemaps in (c) and (d), the LiDAR data is 1 m resolution and was taken in 2019 at Warton and 2017 at Tillingham (the closest dates to the time of sampling at each marsh). The LiDAR colour scheme was thresholded to HAT (5.97 m at Warton, 3.08 m at Tillingham) and LAT (−3.39 m at Warton, −1.63 m at Tillingham) to highlight the marsh platform topography. LiDAR data downloaded from https://environment.data.gov.uk/DefraDataDownload/?Mode=survey. The symbols representing the sampling sites are the same in (c) and (d). The sea wall shapefiles use OS VectorMap™ district SHAPE data (contains OS data © crown copyright and database right 2018)

0.8–1.4 m (ca. 3.5–4.1 m ODN). Such water levels would have exposed the marsh surface to hydrostatic forces (the force induced by water loading on the submerged marsh surface) of up to 14 kPa. However, the relatively rapid (minutes to hours) application of this hydrostatic force means that no vertical deformation would be expected, unless full hydraulic disconnectivity were to occur at the marsh surface.

2.2 | Warton marsh

Warton marsh is located in Morecambe Bay (Figure 1), Northwest England and reaches 1 km wide. The marsh margin consists of a 2 m-high cliff, fronted by blocks of former marsh material. Often the vegetated layer is stripped back up to 5 m landward from the marsh edge (Figure 2). Tidal flats extend up to 3 km seaward. Between 1845 and the early 1970s, Morecambe Bay marshes have undergone alternating phases of erosion and expansion within an overall trend of increasing marsh extent (Gray, 1972; Mason et al., 2010; Pringle, 1995). However, in the past 10 years Warton marsh has retreated by 150–200 m (B. Evans, personal communication, 2019).

Warton marsh sediments are sand/silt-dominated (Ford et al., 2016). Whilst grasses, including *Festuca rubra* and *Agrostis stolonifera*, are common at higher elevations, the marsh is dominated by a close, sheep-grazed sward of *P. maritima*, particularly towards the seaward marsh edge.

At Heysham (Figure 1), the Mean Spring Tidal Range is 8.49 m. The marsh edge elevation is 5.58 m ODN. Warton marsh only floods when water levels approach the Highest Astronomical Tide (HAT; 5.97 m ODN at Warton marsh), or when onshore storm surges elevate water levels above predicted tidal levels (<1% of the time). The HAT results in marsh edge water depths of 0.39 m, so would apply 3.90 kPa hydrostatic pressure. The wave climate in Morecambe Bay (see Figure 1) at 10 m water depth between 2011 and 2020 was dominated by moderate waves (H_s < 0.8 m) and is bimodal, with most waves arriving from the southwest and some lower waves arriving from the northeast (based on data from the Morecambe WaveRider buoy, obtained from Channel Coast Observatory).

3 | METHODS

3.1 | Field sampling

Four sites within each marsh were selected (reflecting the full range of elevations found at each marsh): a tidal flat site, marsh edge site, creek edge site and inner marsh site (Figures 1c and d). Field sampling was undertaken on 17–19 July 2017 and 28 September–1 October 2017 at Tillingham and 6–10 July 2018 at Warton. In July at Tillingham the conditions were relatively dry, but antecedent rain conditions in September resulted in a wetter substrate. The conditions during the Warton sampling were particularly dry.

Bulk samples (weighing approximately 500 g) were taken at 0–10, 10–20 and 20–30 cm depth at all four sites within each marsh, with three additional samples taken at 30–40, 40–50 and 50–60 cm depth at the marsh edge.

FIGURE 2 Photographs of the cliff at Warton (a, b), with (b) showing how vegetation has been stripped back at the top of the cliff and failed blocks remain at the base of the cliff. (c) Stepped/terraced marsh morphology at Cartmel marsh in the north of Morecambe Bay. (d) A characteristic creek with slumped blocks at Warton. Photos taken in July 2018 (a) by B. Evans, October 2018 (b, d) and March 2017 (c) by H. Brooks

'Undisturbed' samples were taken at 0–30 and 30–60 cm depth at each marsh edge site and also at 0–30 cm depth at each tidal flat site. The sampling procedure followed the block sampling method described in BS5930:2015 (BSI, 2015) and is depicted in Figure 3. While it is recognized that no sample can be fully undisturbed, this method is known to minimize disturbance as much as possible compared to other methods (see Carr et al., 2020) and samples were therefore suitable for geotechnical testing. All samples were stored at 5°C prior to analysis.

Undisturbed shear box samples were extracted in a purpose-built open-ended metal sampling box, produced at the British Geological Survey (BGS), with dimensions of 200 mm × 200 mm × 100 mm and sample walls <2 mm thick. Undisturbed one-dimensional oedometer samples were sampled directly into their test ring in the field, except for on the tidal flat where the high water content meant that material was subsampled from undisturbed cylindrical samples in the laboratory. The test rings measured 75 mm in diameter and 20 mm in height.

3.2 | Characterizing substrate composition

Particle size analysis was undertaken on all bulk and undisturbed samples. Organic matter was removed by treatment with 30% w/v hydrogen peroxide overnight and subsequent heating to 90°C in a water bath for minimum 2 h. Sodium hexametaphosphate (4.4% concentration) was used as a deflocculating agent. Samples were analysed using a Malvern Mastersizer 2000. The D_{10}, D_{50} (median) and D_{60} grain sizes were used to quantify the uniformity coefficient (U_c, defining the range of particle sizes) following Knappett and Craig (2012):

$$U_c = \frac{D_{60}}{D_{10}} \quad (1)$$

where D_{60} = 60th percentile grain size (μm), D_{10} = 10th percentile grain size (μm).

To determine the root mass content, 500 g samples were wet sieved through a 425 μm sieve to separate out the roots. The residue (root mass) was then left in an oven at 40°C overnight and the sediment dried at 105°C until the masses remained constant between successive measurements. Root mass content was calculated using

$$m_{roots} = \left(\frac{m_{residue}}{m_{totaldry}}\right) \times 100 \quad (2)$$

where m_{roots} = root mass content as a percentage of dry mass (%), $m_{residue}$ = sieve residue (roots) mass after drying at 40°C (g), $m_{totaldry}$ = total dry root mass and dry sediment mass (the latter after drying at 105°C) (g). Some studies have heated the roots at 60°C (Howes & Teal, 1994), while others have air dried the material (Ouyang et al., 2017). This study found a balance between the drying speed, while minimizing the loss of volatile root components, which can occur at higher temperatures (Hackney & de la Cruz, 1980).

3.3 | Strength and compressibility testing

Geotechnical tests of direct shear strength, residual shear strength and compressibility were undertaken in the geotechnical soils laboratory at the BGS using a shear box, ring shear and oedometer.

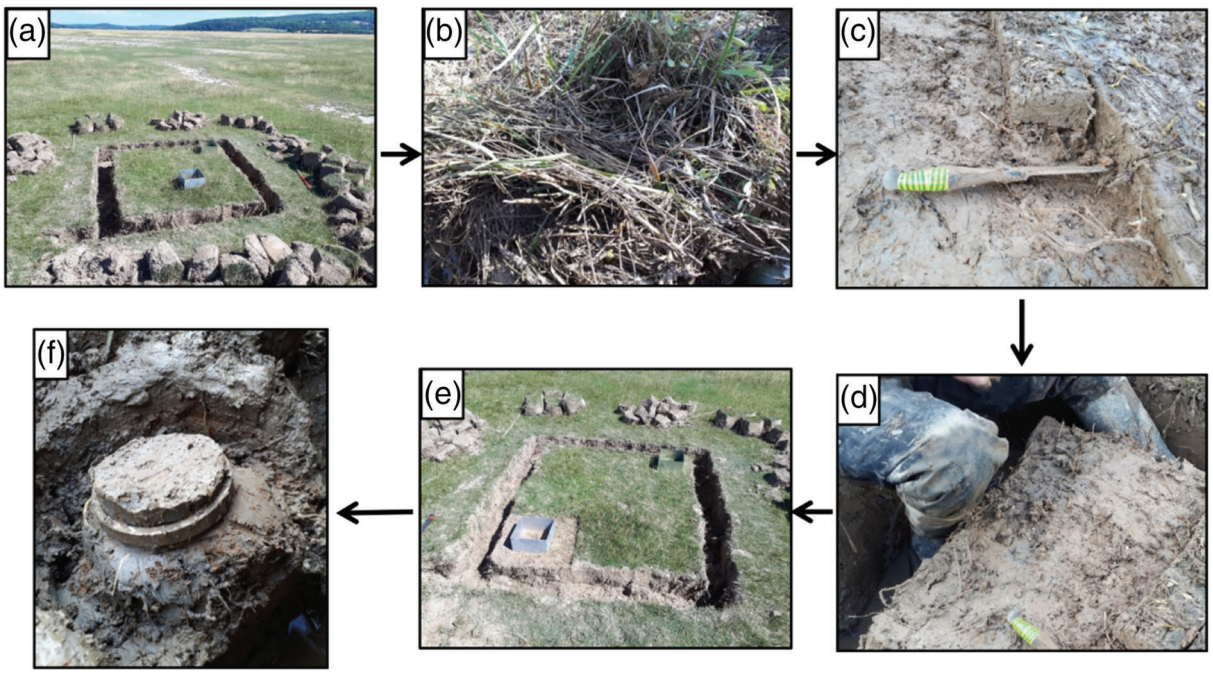

FIGURE 3 Undisturbed sampling method. Initially, a trench the width of a spade was dug around the sampling area (a), then the vegetation was cut back (b) and the upper 2–5 cm of sediment were removed (c) to leave a level plinth (d). The sampler was then placed on the plinth and the excavation began (e) until 2 cm of sediment protruded above the sampler (f). Photos taken by H. Brooks in September 2017 (b, c and f) and July 2018 (a, d and e)

3.4 | Shear box

Shear box and ring shear tests can record the drained strength of soils (i.e. where the rate of changes in total applied stress is slower than the rate of dissipation of excess pore water pressure). Therefore, they provide vital information on the response of the marsh substrate to cumulative long-term changes in the total applied stress (longer than approximately a week, or the time over which it takes excess pore water pressures to dissipate). Theoretically, changes in the applied stress could relate to stress changes induced by erosion of the overburden (although such surface erosion is known to be negligible on salt marsh surfaces; Spencer et al., 2015), or changes in the elevation of the water table. The effect of these longer-term processes is rarely considered in salt marsh studies. Therefore, while this paper does not intend to mimic real-world erosion processes, it aims to understand the behavioural properties of marsh substrates, while incorporating other, rarely studied methods of stress application. Shear box and ring shear tests were therefore performed on the samples to understand factors which may be contributing to substrate strength and to understand the influence of the longer-term stress environment (e.g. from changes in the water table), rather than to indicate when and why particular erosion processes might occur.

Undisturbed field samples were subsampled in the laboratory to fit flush to a 100 mm × 100 mm × 20 mm shear box, following the undisturbed sampling technique in Figure 3. Each full shear box test required three duplicate specimens, which were restrained laterally by the apparatus, subjected to a vertical load and then sheared along a horizontal plane. Specimens were consolidated overnight and sheared the following day, then replaced with the next specimen for the next test stage. All tests were undertaken using a Wykeham Farrance Model No. 25402 shear box.

The shear box test method followed the consolidated/drained method in BS1377–7 (BSI, 1990a) and Head (1994). Samples were saturated using distilled water and the shear rate for each test stage was dictated by T_{100} (the time at which the sample would reach 100% consolidation, assuming that the consolidation rate during primary consolidation continued throughout the test; Bishop & Henkel, 1962). The precise shear rate was determined by first using T_{100} to calculate the maximum time to failure (t_f), based on Gibson and Henkel (1954):

$$t_f = 12.7T_{100} \tag{3}$$

where t_f = time to failure (min), T_{100} = theoretical time to 100% consolidation (min).

The likely horizontal shear deformation (mm) of the sample at the point of failure was then found based on values in Head (1994) for the sediment type in question. Likely horizontal shear deformation was therefore taken to be 10 mm for samples from Tillingham (a plastic clay) and 2 mm for samples from Warton (a dense sand). This likely horizontal shear deformation was divided by t_f to give the maximum displacement rate (mm/min) for use in the test. This displacement rate was between 0.001 and 0.1 mm/min, in accordance with Bolton's (1991) recommendations for clay and silt-dominated substrates under fully drained conditions. The displacement rate was therefore sufficiently slow to allow drainage and prevent the build-up of excess pore water pressure, allowing the assumption of zero pore water pressure and constant vertical effective stress, σ_n', throughout each test. The test was therefore a drained test where σ_n' is equal to the total stress, σ_n. Although the samples were taken from <60 cm depth, the applied vertical stress was restricted by the minimum stress which could be applied in the shear box. Vertical total stresses (σ_n) therefore started at 10 kPa for the first specimen, increasing to 20 and 40 kPa for the second and third specimens. This typified effective stresses equivalent to 1, 2 and 4 m water overburden (assuming full hydraulic disconnectivity and rapid dissipation of pore water pressures), or approximately 0.5, 1 and 2 m sediment overburden, respectively.

The shear stress (τ, kPa), applied to the shear surface at all times throughout the shear stage, was calculated using

$$\tau = \frac{P}{A} \times 1000 \tag{4}$$

where P = horizontal shear force (load ring calibration multiplied by load dial reading, N) applied to the specimen and A = initial plan area of the specimen (mm^2).

Stress–strain curves were produced from which the peak shear strength (τ_f, kPa) was derived. Where the material did not reach τ_f, the final shear stress reached was taken as τ_f. The derived τ_f values for each specimen were then plotted against vertical effective stress (σ_n, kPa) to construct a failure envelope determined by the Mohr–Coulomb equation:

$$\tau_f = c' + \sigma_n' \tan\varphi' \tag{5}$$

where τ_f = shear strength (kPa), c' = effective cohesion (kPa), σ_n' = vertical effective stress (kPa), φ' = effective angle of shearing resistance (°). The values of φ' and c' were calculated from the failure envelope.

3.5 | Ring shear

The ring shear apparatus comprised an annular cell (height = 5 mm, inner radius = 35 mm, outer radius = 50 mm). Ring shear samples were prepared from the trimmings of the second shear box specimen for each location/depth. Trimmings at their natural moisture content were sieved at 1.18 mm to remove most roots and any larger particles, in accordance with BS1377–7 (BSI, 1990a). The sample was carefully smeared into the annulus using a thin-tipped palette knife, saturated with distilled water and consolidated at the lowest vertical total stress (14.4 kPa).

The test procedure followed BS1377–7 (BSI, 1990a; Head, 1994) and was undertaken using the lowest vertical total stresses allowed by the machine (14.4, 26.6 and 51.1 kPa for stages one, two and three, respectively). The same sample remained in the apparatus for all three consolidation and shear stages, so only one sample was needed to obtain all three peak shear strength values.

After each stage, the average shear stress (τ, kPa) applied over the shear plane was calculated using

$$\tau = \frac{3L(F_1 + F_2)}{4\pi(r_2{}^3 - r_1{}^3)} \tag{6}$$

where L = distance between the two points of force application on the tension beam (mm), F_1 = final force on dial 1 (N), F_2 = final force on dial 2 (N), r_1 = inner radius of test specimen (mm), r_2 = outer radius of test specimen (mm).

As residual cohesion is assumed to be zero (Lupini et al., 1981; Tiwari & Marui, 2005), the residual strength was determined from

$$\tau_r = \sigma_n' \tan(\varphi_r') \quad (7)$$

where τ_r = residual shear strength (kPa), σ_n' = vertical effective stress (kPa), φ_r' = residual angle of effective shearing resistance (°).

The residual angle of effective shearing resistance was calculated as in the shear box test.

3.6 | Oedometer

Samples were tested on a GDS Automatic Oedometer System (GDS Instruments Ltd, 2014). Tests were undertaken in accordance with BS1377–5 (BSI, 1990b) and Head (1994), and duplicate tests were run on two 'replicate' samples from each undisturbed sampling location, where possible. Samples were saturated with distilled water.

The one-dimensional consolidation test was run as an eight-stage axial (vertical) load–unload test comprising six consolidation stages, with a maximum load of 400 kPa, followed by two unloading stages (Table 2). Each test stage lasted 24 h.

Following each loading stage, the cumulative final displacement (d_f, mm) was noted from the gauge, with a positive value denoting compression. As such, d_f following each stage was equal to the cumulative height change since the start of the test, ΔH (mm). This allowed the calculation of the cumulative void ratio change from the start of the test (Δe), using

$$\Delta e = \frac{\Delta H}{H_s} \quad (8)$$

where H_s = equivalent height of solid particles (mm).

From this, the new void ratio at the end of a loading stage (e), defined as the initial void ratio (e_0) minus the change in void ratio (Δe), could be calculated:

$$e = e_0 - \Delta e \quad (9)$$

TABLE 2 Summary of the stage type and applied pressure throughout the oedometer test

Stage number	Stage type	Pressure applied (kPa)
1	Swell	n/a
2	Consolidation	12.5
3	Consolidation	25
4	Consolidation	50
5	Consolidation	100
6	Consolidation	200
7	Consolidation	400
8	Unload	200
9	Unload	1

The overall results of each test were displayed as graphs of void ratio (e) against vertical effective stress (σ'). The e–$log\ \sigma$' relationship was used to derive the maximum previous stress to which the sediment had been subjected. This was then used to determine the over-consolidation ratio (OCR; see Knappett & Craig, 2012) using Equation (10). This highlighted whether structural changes due to applied effective stress would be reversible or irreversible:

$$\mathrm{OCR} = \frac{P_c}{P_0} \quad (10)$$

where P_c = maximum previous vertical effective stress to which the soil has been subjected (pre-consolidation pressure, kPa), P_0 = *in-situ* effective stress (kPa) to which the soil was exposed upon excavation.

4 | RESULTS

4.1 | Substrate composition

Particle size distributions at Tillingham were platykurtic to mesokurtic (kurtosis = 0.79–0.91), while distributions at Warton were very leptokurtic (kurtosis = 1.89–2.03). D_{50} was higher ($p = 0.009$) at Warton (D_{50} = 53.62–85.86 μm) than at Tillingham (D_{50} = 5.84–67.00 μm), whereas U_c was higher ($p = 0.028$) at Tillingham (mean = 13.00) than at Warton (mean = 6.00), based on the Kruskal–Wallis test (Kruskal & Wallis, 1952).

Root mass content was higher and more variable at Tillingham (mean = 0.78%; 1 SD = 0.61%) than at Warton (mean = 0.23%; 1 SD = 0.30%). While root mass at Warton decreased clearly with depth, the change in root mass was less consistent with depth at Tillingham (Figure 4).

4.2 | Shear behaviour

Stress–strain curves indicated that the substrate at both Tillingham and Warton required constant application of shear stress to produce deformation (Figure 5), although the substrate begins to deform within seconds of the stress being applied. Mohr–Coulomb failure envelopes from the shear box tests denoted a low c' (<7.0 kPa) at both sites (Table 3). The φ' was higher at Warton than Tillingham for all equivalent locations, ranging between 29.9 and 36.1° at Tillingham, but between 33.4 and 43.5° at Warton (Table 3).

At both sites, the difference between φ' and φ_r' was greatest at 0–30 cm depth at the marsh edge site (Table 3), and the difference was greater at Warton marsh edge (0–30 cm depth; 43.5°) than at Tillingham (35.3°; Table 3).

Throughout the range of vertical effective stresses applied in the shear box test, the Warton marsh edge samples had a higher shear strength than the equivalent Tillingham samples (by up to ca. 15 kPa). However, for the ring shear test, this difference in strength between the Tillingham and Warton marsh edge samples was reduced, with samples from both sites having a comparable shear strength (within ~5 kPa) for a given vertical effective stress. The shear strengths of the tidal flat samples were comparable to within ca. 5 kPa. As

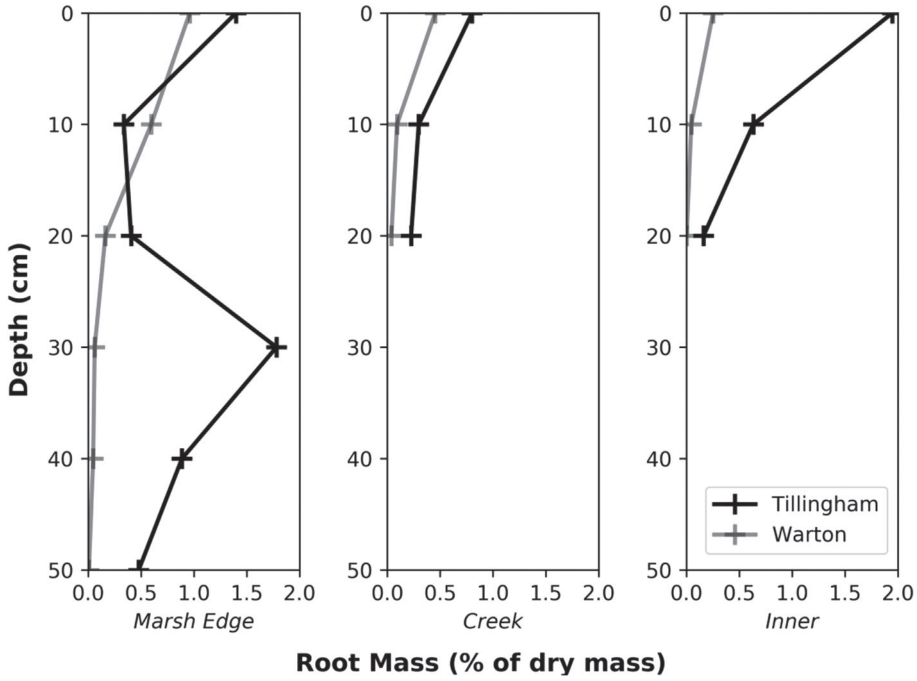

FIGURE 4 Root mass variation with depth at both Tillingham and Warton. Samples are plotted as the depth of the upper limit of the sample (e.g. 0–10 cm sample is plotted at 0 cm)

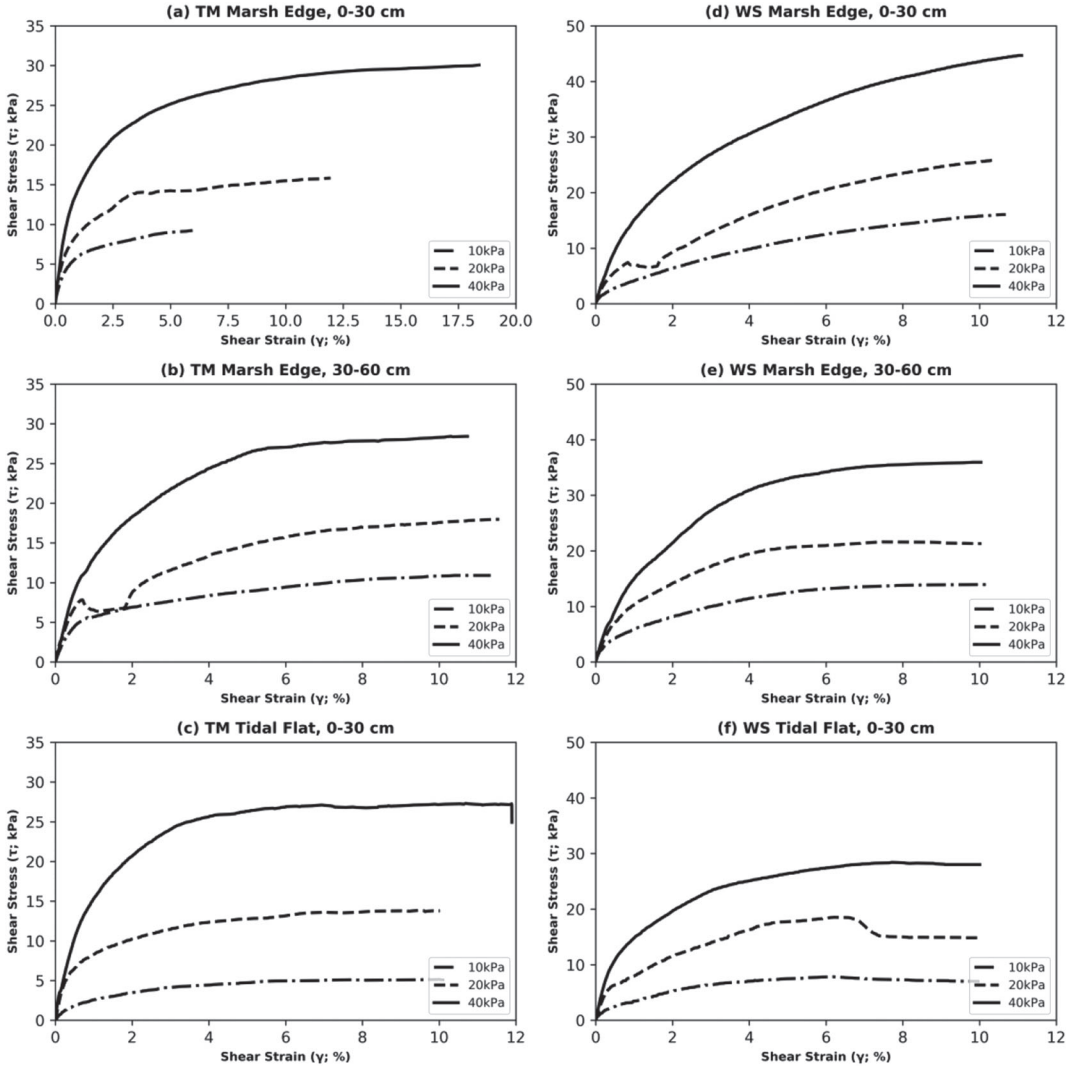

FIGURE 5 Stress–strain curves for Tillingham (a–c) and Warton (d–f) shear box samples

TABLE 3 Angle of internal friction (φ', °), effective cohesion (c', kPa) and residual angle of internal friction (φ_r', °), as determined by shear box and ring shear tests. The difference between the angle of internal friction and the residual angle of internal friction (φ' − φ_r') is also shown. All values are given to one decimal place

	Tillingham			Warton		
	Marsh edge, 0–30 cm	Marsh edge, 30–60 cm	Tidal flat, 0–30 cm	Marsh edge, 0–30 cm	Marsh edge, 30–60 cm	Tidal flat, 0–30 cm
Angle of internal friction (°)	35.3	29.9	36.1	43.5	36.1	33.4
Cohesional strength component (kPa)	2.1	5.7	0	6.6	6.8	2.9
Residual angle of internal friction (°)	29.4	29.2	32.4	31.2	32.3	29.2
Change in angle of internal friction (°)	5.9	0.7	3.7	12.3	3.8	4.2

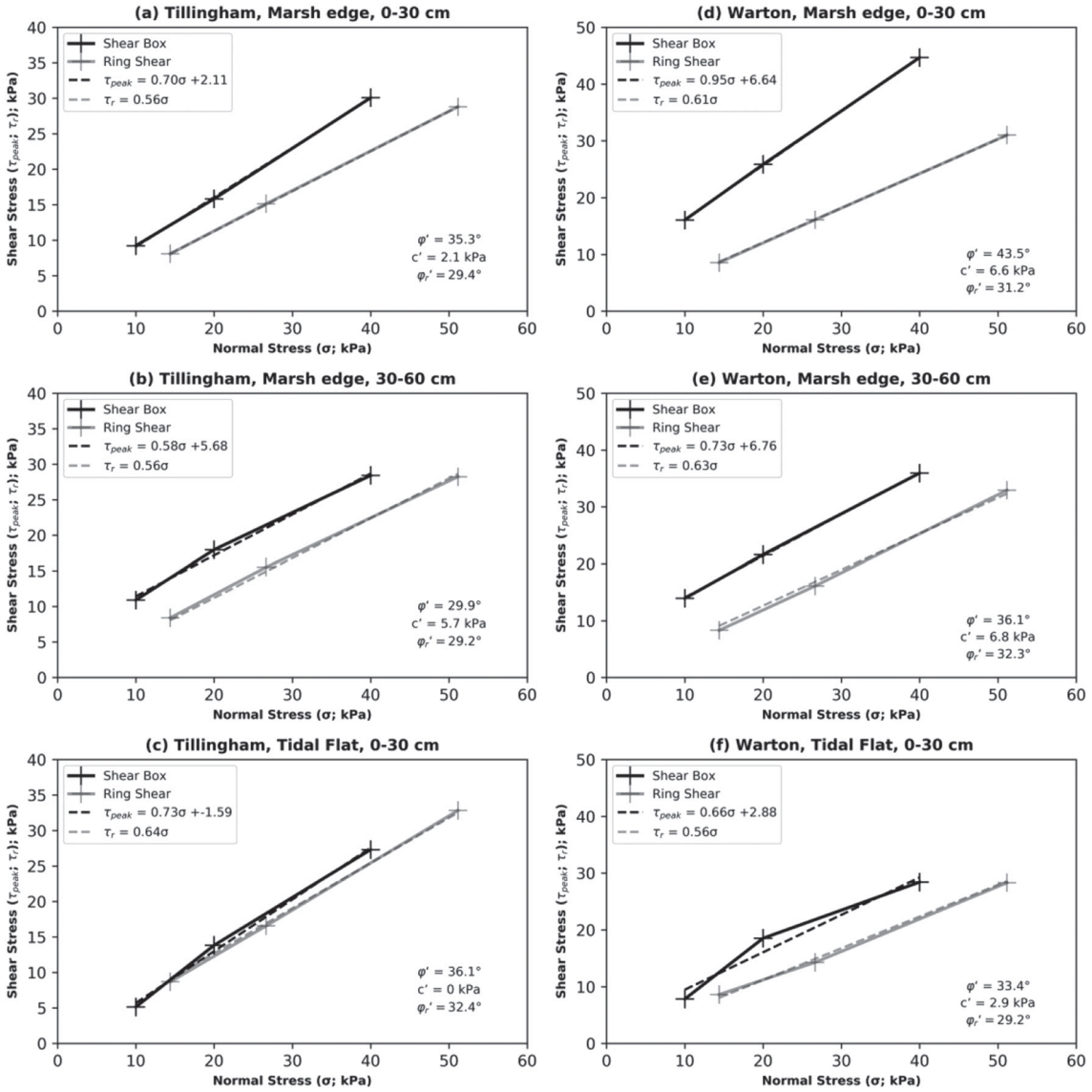

FIGURE 6 Mohr–Coulomb failure envelopes for shear box and ring shear tests at each site. Angle of internal friction (φ', °), effective cohesion (c', kPa) and residual angle of internal friction (φ_r', °) are also shown. Samples from Tillingham are depicted in (a)–(c), while Warton samples are shown in (d)–(f)

expected, the shear stress a sample could withstand for a given vertical effective stress was lower for the residual strength than for the peak strength by 0.1–25 kPa depending on the sampling location and vertical effective stress (Figure 6). This is denoted by the lower φ_r' compared to φ' at all sites (Table 3).

4.3 | Consolidation behaviour

Tillingham oedometer samples underwent little initial axial (vertical) displacement in each stage (<5 mm), sometimes for up to 3 min after initial effective stress application. The consolidation curve then began

as expected (with slow initial compression, rapid 'primary' compression, followed by slow 'secondary' compression), albeit delayed (Figure 7). At Warton, consolidation in each loading stage occurred rapidly (generally under 5 s) after the initial load application, and samples consolidated less than at Tillingham (Figure 8). For example, after application of the maximum pressure (400 kPa), no Warton samples consolidated by more than 3 mm, while up to just over 8 mm consolidation occurred at Tillingham for the same load (Figures 7 and 8).

The initial void ratio at Tillingham (1.82–2.77) was higher than at Warton (0.98–1.15; Figure 9). During unloading, the Tillingham samples dilated, but the initial void ratio was not reached with any sample and only 51–66% of the initial void ratio was recovered. The Warton samples dilated during unloading, with all samples except those from 30 to 60 cm depth at the marsh edge returning to their initial void ratio (Figure 9).

At Warton, the pre-consolidation pressure was higher, particularly at 30–60 cm depth at the marsh edge, and on the tidal flat. This resulted in a larger OCR at Warton (mean of 10.75, compared to mean of 7.03 at Tillingham; Table 4).

5 | DISCUSSION

5.1 | Shear behaviour in response to applied stress

5.1.1 | Cohesional strength and angle of internal friction

The effective cohesional strength (*c*') was low, varying in the range 0.0–5.7 kPa at Tillingham and 2.9–6.8 kPa at Warton (Table 3). In comparison, riverbank cohesion has been measured at 15 kPa on the Latrobe River, Australia (Abernethy & Rutherfurd, 2000) and 8.3 kPa on the Nepean River, Australia (Docker & Hubble, 2008). Cohesion in sandy loam agricultural soils also tends to be higher, with Mouazen (2002) recording cohesion of 5.7–35.9 kPa over a range of dry bulk densities. For samples comprising primarily sediment, this low cohesional strength would largely reflect the electrostatic forces between platy clay particles and therefore suggest that the substrate derived little strength from its clay mineral content. Polvi et al. (2014) report cohesion in sandy loam soils as low as 2.4 kPa, with

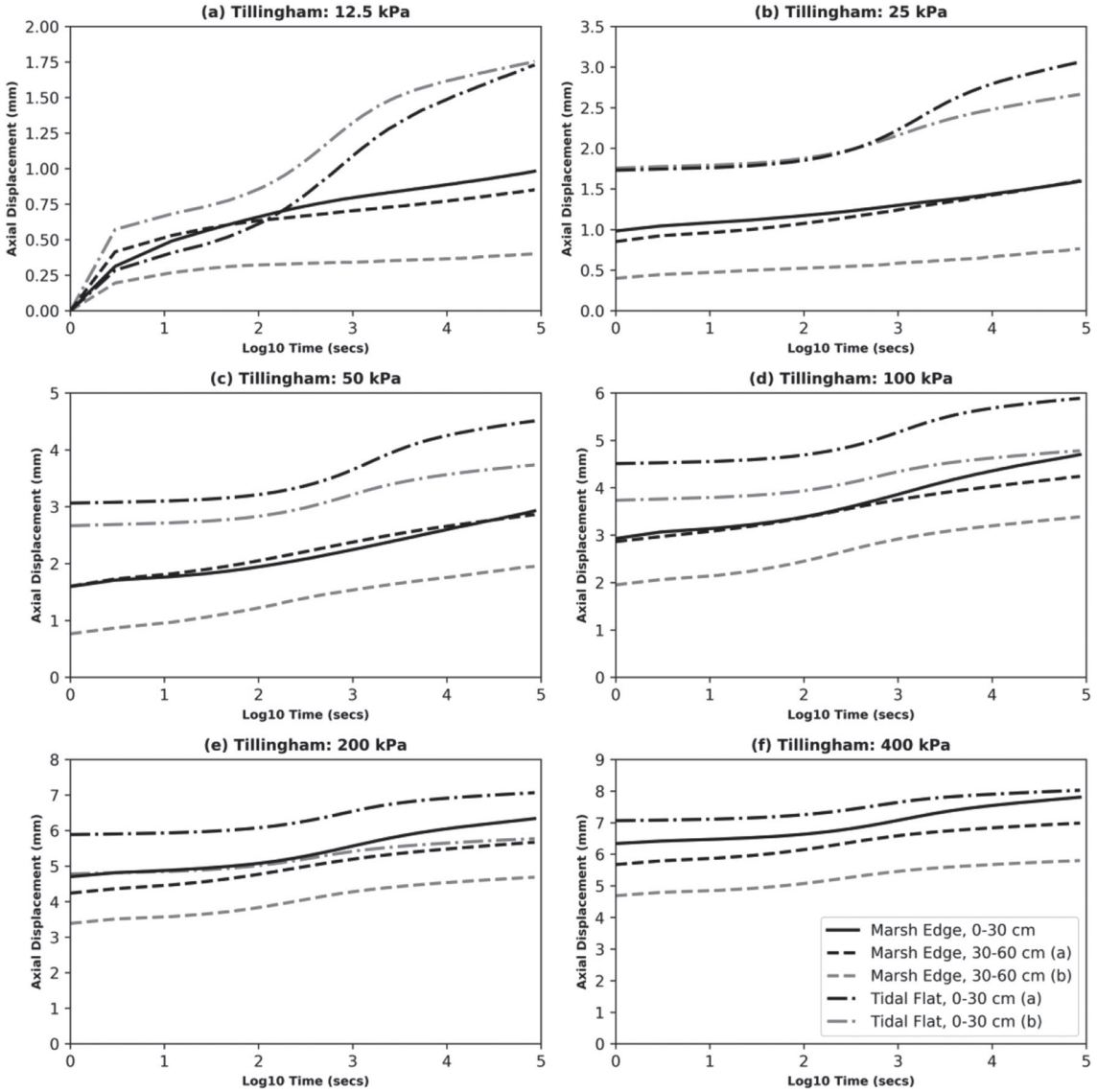

FIGURE 7 Time (log_{10} [s]) vs. axial (vertical) displacement (mm) for all five samples at Tillingham. Graphs relate to the consolidation stage, and thus the applied shear stress: 12.5 kPa (a), 25 kPa (b), 50 kPa (c), 100 kPa (d), 200 kPa (e) and 400 kPa (f)

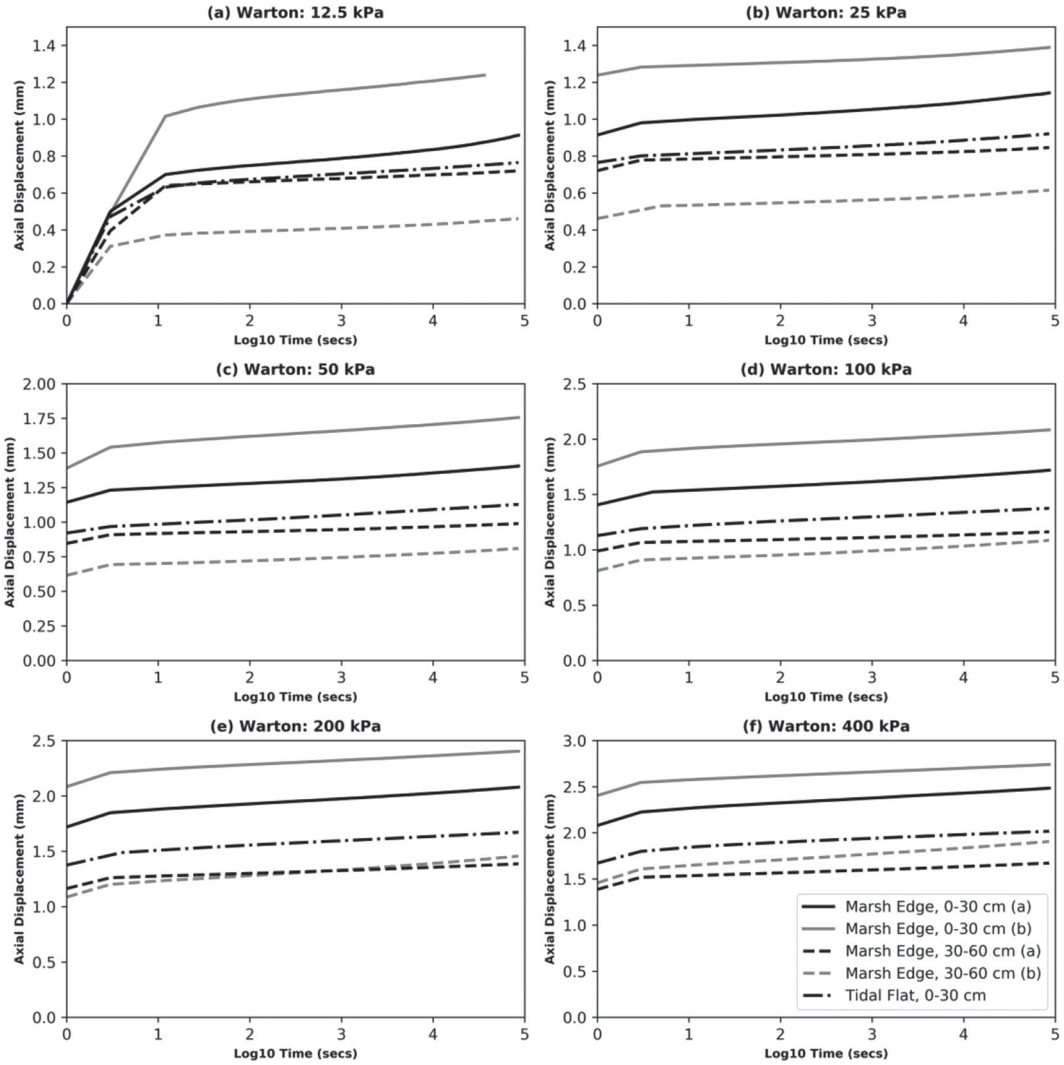

FIGURE 8 Time ($\log_{10}$ [s]) vs. axial (vertical) displacement (mm) for all five samples at Warton. Graphs relate to the consolidation stage, and thus the applied shear stress: 12.5 kPa (a), 25 kPa (b), 50 kPa (c), 100 kPa (d), 200 kPa (e) and 400 kPa (f)

considerable increases in cohesion due to the presence of roots. However, the salt marsh samples used here contained not only roots but likely also macropores, which are known to be related to a lower shear strength at these sites (Chirol et al., 2021) and the interpretation of results is necessarily more complicated.

The angle of internal friction (φ') and residual angle of internal friction (φ_r') were 29.9–36.1 and 29.2–32.4° at Tillingham and 33.4–43.5 and 29.2–32.3° at Warton, respectively. The higher frictional strength at Warton likely results from its coarser grain size relative to Tillingham. These values are at the upper end of φ' measurements on riverbanks: $\varphi' = 16°$, LaTrobe River, Australia (Abernethy & Rutherfurd, 2000); $\varphi' = 27–28.5°$, Goodwin Creek, Mississippi, USA (Simon & Collison, 2002) and in agricultural sandy loam soils: $\varphi' = 24.9–36.9°$ (Mouazen, 2002).

Few other studies report c' and φ' for salt marsh sediments. Francalanci et al. (2013) measured φ' as 17.7, 30.6 and 32.9° at three marsh edge locations in the Venice Lagoon, which had a corresponding c' of 10.8, 8.0 and 5.3 kPa. These samples were predominantly silt (69–84%), with a secondary clay component (13–28%) and a smaller sand component (<5%). The latter two samples displayed a similar φ' and c' to those found at Tillingham and Warton, while the first sample had a lower φ' and slightly higher c'. Only one other marsh/tidal flat has been tested using shear box and ring shear tests: Bothkennar, Scotland. The results presented here are comparable to estuarine silts at Bothkennar, where $c' = 1.5$ kPa, $\varphi' = 34°$ and $\varphi_r' = 30°$ (Hight et al., 2003; Lehane & Jardine, 1992). The angle of shearing resistance for both peak and residual values was therefore high at the Venice Lagoon, Bothkennar, Warton and Tillingham, in the context of known φ' and φ_r' values in the geotechnical literature. This may indicate a high angular grain content and low platy clay content (Giang et al., 2017). However, these studies did not discuss the relevance of these results for marsh stability further.

The higher φ' at Warton reflects the lower void ratio (Figure 9) and results in a consistently higher shear strength at Warton than at equivalent locations at Tillingham. A lower void ratio increases φ' because it indicates a higher packing density, more interparticle contacts and greater interlocking between particles (Barnes, 2010). While both larger particle sizes and a higher U_c (the latter not a characteristic of Warton sediments) have been shown to increase the φ' and thus the peak substrate strength (Alias et al., 2014; Kara et al., 2013), not all studies reach the same conclusion (e.g. Latha & Sitharam, 2008).

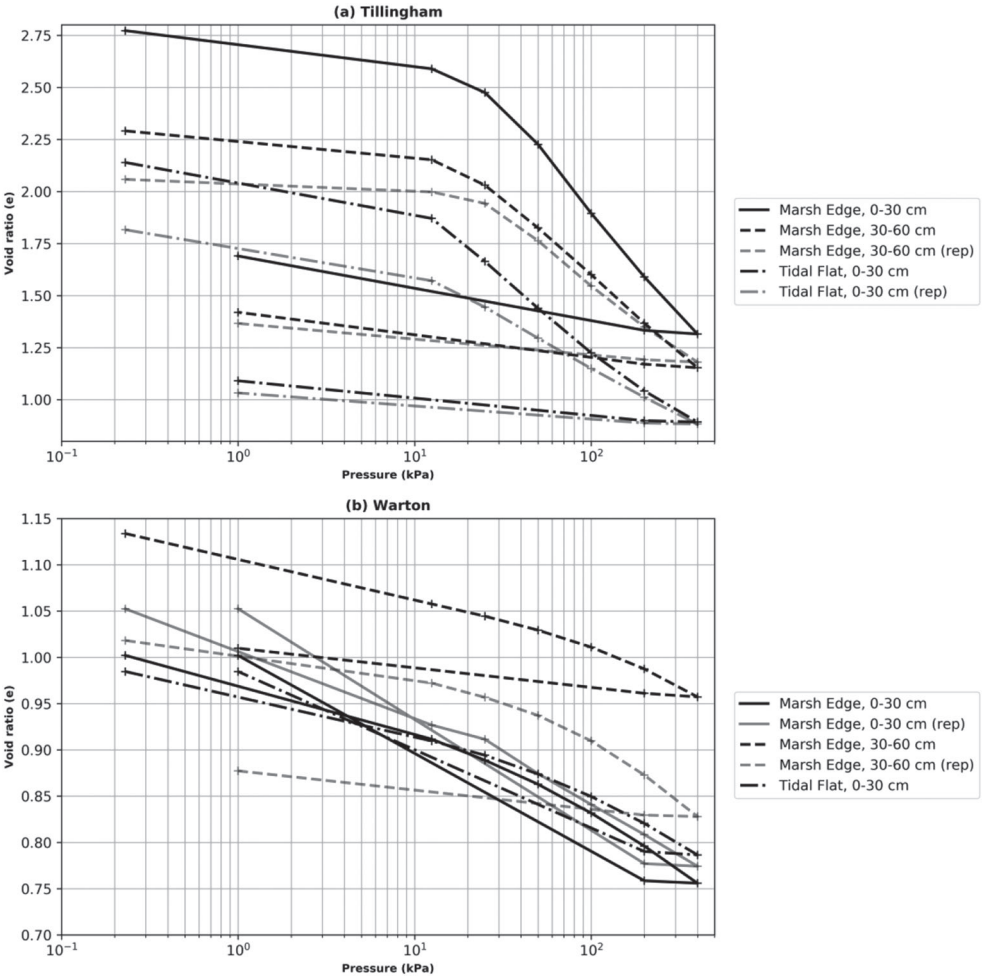

FIGURE 9 Pressure applied (kPa) vs. void ratio (*e*), where a higher void ratio indicates a lower bulk density at the end of each stage for samples from Tillingham (a) and Warton (b)

Rather, many studies infer that the void ratio may be the most important influence on φ', with larger particle sizes and a higher U_c both reducing the void ratio (Latha & Sitharam, 2008; Selig & Roner, 1987). For example, Vangla and Latha (2015) note that particle size does not affect peak shear strength when the initial void ratio remains constant. This paper therefore supports existing research (Crooks & Pye, 2000; Crooks et al., 2002), which uses separate density and undrained shear strength methods, in finding that a lower void ratio (or higher bulk density) increases the shear strength of marsh substrates.

At Warton, the higher φ' on the marsh surface compared to φ' at depth likely reflects compaction of the upper marsh stratigraphy, possibly due to grazing (e.g. Lambert, 2000). Compaction increases grain interlocking and friction between particle contacts, leading to higher values of φ' (Barnes, 2010). Grazing-induced compaction may therefore locally increase the substrate shear strength in the uppermost layers. While some autocompaction may occur in deeper sediment layers (Allen, 1999), the results of this study are consistent with studies elsewhere that have shown that grazing-induced compaction at depth (below 20 cm) can be negligible or absent (Elschot et al., 2013). The higher φ' on the marsh surface compared to φ' at depth could also be related to changes in moisture content and therefore pore water pressure, caused by root suction, desiccation or reductions in the level of the water table. However, further research would be needed to assess the relative influence of compaction and changes in moisture content on φ'.

5.1.2 | Peak and residual shear strength

Substrates can demonstrate a reduction in strength following previous failure, usually reflecting clay softening/reorientation to the failure plane (Knappett & Craig, 2012). This was not the case in the substrates tested here, as there was no reduction in τ past the point at which the maximum strain was reached (Figure 5). However, the Mohr–Coulomb failure plots (Figure 6) showed a difference between the peak and residual scenarios, with the residual strength for a given vertical effective stress always being lower in the residual scenario. As the 'characteristic' fall to residual strength is not noted in the stress–strain curves, but a reduction in strength is recorded in the Mohr–Coulomb failure envelopes, this implies that the shear box and ring shear tests could be recording a different property affecting substrate strength. For example, this reduction in strength could be due to the remoulding of samples or the removal of roots during sample preparation.

The shear box test (measuring peak strength) reflected an undisturbed sample with intact roots, whereas the ring shear sample (measuring residual strength) comprised only the reconstituted sediment component of the substrate, with minimal roots present. The observed reduction in strength from the peak to the residual scenario (Figure 6) thus appears to reflect the removal of strength provided by roots. Comparing φ_r' and φ' thus begins to separate the influence of clay softening/reorientation from that of root presence. The fact that the largest decrease in φ' from the peak to the residual scenario at

TABLE 4 Overburden pressure, pre-consolidation pressure and overconsolidation ratio (OCR) for oedometer samples. Pre-consolidation pressure is only given to the nearest integer due to the subjectivity involved with calculating the pre-consolidation pressure

	Tillingham					Warton				
	Marsh edge, 0–30 cm	Marsh edge, 30–60 cm (a)	Marsh edge, 30–60 cm (b)	Tidal flat, 0–30 cm (a)	Tidal flat, 0–30 cm (b)	Marsh edge, 0–30 cm (a)	Marsh edge, 0–30 cm (b)	Marsh edge, 30–60 cm (a)	Marsh edge, 30–60 cm (b)	Tidal flat, 0–30 cm
Overburden pressure (kPa)	2.04	6.66	6.87	2.33	2.39	2.12	2.27	7.17	7.23	2.77
Pre-consolidation pressure (kPa)	27	21	27	17	18	27	23	65	52	42
OCR	13.25	3.15	3.93	7.29	7.54	12.17	10.14	9.07	7.19	15.17

both Tillingham and Warton occurred at the marsh surface (Table 3), where root mass was greatest (Figure 4), corroborates the hypothesis that roots are contributing to this loss of frictional strength.

The ability to isolate the strength provided by roots, as demonstrated through the techniques deployed in this study, is key to identifying the response of marsh substrates to forcing. While many studies have identified the role of roots in increasing the strength of the uppermost marsh substrate layer (e.g. Bendoni et al., 2014, 2016; Van Eerdt, 1985a), no studies have previously isolated the strength derived from roots in a three-dimensional salt marsh substrate sample. This research gap has limited our ability to understand the link between marsh edge erosion processes and retreat rates.

Previous studies have explored the tensile strength of the roots in vegetated substrates, and found that this may reflect vegetation density and type (Van Eerdt, 1985a) and that it affects the morphology of tension cracks which are narrower and shallower than in unvegetated substrates (Francalanci et al., 2013). Van Eerdt (1985b) measured the tensile strength provided by two salt marsh species in Oosterschelde, The Netherlands, finding that *S. anglica* provided greater tensile strength than *L. vulgare*. Van Eerdt (1985b) argued that the contribution of roots to substrate strength is proportional to the number of roots intersecting the failure plane. As such, the fine but dense root mat resulting from *Puccinellia* spp. at Warton would be expected to provide greater strength to the substrate than the less dense but thicker roots from the mixed species canopy dominated by *A. portulacoides* and *Elymus athericus* at Tillingham. This agrees with the higher peak strength recorded in the Warton substrates for a given vertical load, compared to Tillingham (Figure 6), and also the fact that the greatest reduction in frictional strength between the peak and the residual scenarios occurred at 0–30 cm depth at Warton but not at Tillingham. Similarly, roots are known to contribute more to the shear strength of sandy substrates than finer-grained substrates (Lo et al., 2017), again agreeing with the greatest decrease in strength from the peak to the residual scenario occurring at Warton. Subjecting salt marsh soils to geotechnical methods thus contributes towards our understanding of the relative additional strength provided by roots, which has important implications for understanding of marsh edge erosion processes.

Isolating the role of roots in providing strength to substrates has implications for modelling the future landform evolution of salt marshes, particularly at the scale of an individual marsh. Salt marsh evolution models often include only an 'erodibility coefficient' to incorporate marsh substrate strength or assume that the substrate is vertically homogeneous (e.g. Bendoni et al., 2014; Mariotti & Carr, 2014). The lack of geotechnical measurements for informing models of marsh edge erosion by mass wasting was noted 10 years ago by Mariotti and Fagherazzi (2010) and there has been little additional data since then. The research presented here has demonstrated that the relative influence of different factors (e.g. root mass) on shear strength varies with substrate depth, with the influence of roots being high in the upper substrate layer. Introducing a two-layered substrate to models of specific erosion processes (e.g. toppling failure; Bendoni et al., 2014), with the resistance of the upper layer reflecting the combined strength of the sediment matrix and roots, while the lower layer reflects the sediment matrix and some partially decomposed roots (see Brooks et al., 2021) would improve models of future marsh evolution. Our results illustrate that the assumption of vertical uniformity

of resistance to physical stress is not justified, particularly where roots contribute to upper layer shear strength.

The results presented here give an insight into the relative difference in strength between the upper and lower layers of marsh substrate at Tillingham and Warton, with the difference in strength being greater at Warton. This strength difference between the two layers could be modified for marsh evolution models at specific sites, depending on the type of vegetation present (and therefore the number of roots intersecting the failure plane and other factors).

Future marsh evolution models should incorporate such vertical variations in shear strength and recognize the relative contributions made by root systems. Pollen and Simon (2005) and Simon and Pollen (2006) developed a model for the prediction of critical conditions for riverbank stability on the basis of vertically varying controls (e.g. sediment and vegetation composition) that determine the likely mechanism of failure (e.g. planar or cantilever failure) following undercutting. What is needed now is a similar approach for saltmarsh margins. We have considerable data on the critical erosion shear stress of marsh substrates (e.g. Watts et al., 2003) and therefore the likelihood and potential rate of undercutting of the marsh platform. However, more geotechnical studies such as that presented in this paper are needed to understand controls on substrate failure type, timing and rate following undercutting, across a range of substrate types, marsh margin morphologies and hydrodynamic settings. Our results can constrain the geotechnical behaviour of individual marsh sediment layers and, in combination with further empirical evidence for margin failure processes, lead to an improved understanding of the processes involved in marsh margin failure (e.g. tension crack formation and cantilever or toppling failure) and the influence of marsh composition on why certain processes occur. This will ultimately allow the salt marsh community to produce similar failure models to those provided for riverbank failure whereby the Mohr–Coulomb failure envelope is modified to include the root reinforcement of soil strength (e.g. Pollen & Simon, 2005; Simon & Pollen, 2006). Using such a model will allow the vertical extent and rate of undercutting to be varied, and the resulting influence on the failure processes and rates to be compared.

5.2 | Consolidation behaviour

One mechanism of wetland elevation change (in particular in response to storms) is the process referred to by Cahoon (2006) as 'soil shrinkage', which refers to the expulsion of water from voids within the soil. In the geotechnical engineering literature, this is known as 'consolidation'. It is important to note that this is distinct from the process of compaction (expulsion of air from voids) or the process of 'autocompaction' noted in salt marshes, with the latter denoting the compression of the substrate under its own weight and accompanying increase in dry density (see Allen, 2000) due to a combination of consolidation (expulsion of liquid) as well as compaction (expulsion of air). This distinction is important as it has implications for the hydraulic conductivity (and therefore drainage) of the soil and must be taken on board by the salt marsh community to achieve accurate interpretation of observed compression of marsh substrates.

5.2.1 | Timing/magnitude of expected displacement

The results of this study show that the rate of marsh substrate response to applied vertical effective stress varies between locations. While axial displacement at Tillingham was delayed (by up to 3 min; Figure 7), it occurred rapidly at Warton following initial load application (generally in under 5 s; Figure 8). This likely reflects the higher permeability of the Warton substrate, caused by the higher sand and lower clay content, allowing faster drainage and consolidation (Head, 1994). The slower consolidation response at Tillingham may reflect resistance provided by roots, which, once crushed, allow consolidation to continue at a faster rate. The composition (organic and minerogenic) of a substrate can therefore influence the rate of the substrate response to applied vertical effective stress.

Samples at Warton consolidated less (up to 15% of initial height) than at Tillingham (up to 45% of initial height). This likely reflects the higher initial void ratio at Tillingham (1.82–2.77) than at Warton (0.98–1.15), and the higher root content at Tillingham. In marsh substrates on the Mississippi Deltaic Plain with organic matter contents of 2.36–5.37% by volume (Nyman et al., 1990), roots retain moisture and often form a macropore structure within the marsh substrate (DeLaune et al., 1994), especially those roots which are hollow, such as *S. anglica* roots. Roots can thus provide a space for water and air, increasing the void ratio. Finally, roots have some elasticity and can be compressed more than solid particles when loaded (Head, 1994). Furthermore, in Cowpen Marsh, Tees Estuary, UK, Brain et al. (2011) found higher compression in samples with open structures linked to higher organic content than for those with lower organic content. The presence of open structures (void space between particles or within roots) therefore affects the magnitude of the salt marsh substrate response to applied vertical effective stress across a range of substrate compositions and marsh locations.

The vertical load applied to a marsh by an increase in water depth during a storm surge depends on both the surge magnitude and the marsh position within the tidal frame. For example, the highest water elevation at Warton based on the Heysham tidal record between 1 January 1964 and 30 April 2020 reached 1.19 m above the marsh surface on 1 February 1983. The duration of this inundation depth is unknown, as the surge damaged the tide gauge. At Tillingham, the highest water elevation from the Harwich tidal record between 1 January 1954 and 30 April 2020 reached 1.28 m above the marsh edge surface on 5 October 1967, for 2–3 h. These 'extreme' storm surges would have applied a vertical total stress of 11.90 and 12.79 kPa at Warton and Tillingham, respectively.

Although the weight of water applies a total vertical stress on the marsh surface, the applied stress will be taken up by additional pore water pressure, and not changes to the substrate structure. The only scenarios which would allow deformation to occur would be if there were full hydraulic disconnectivity at the marsh surface, or if the grain size were large enough to provide free drainage (neither of which is likely to be achieved in salt marsh settings). Therefore, at least at Tillingham and Warton marshes, deformation due to the consolidation process (and therefore the 'soil shrinkage' process referred to in Cahoon, 2006) seems unlikely.

While Cahoon (2006) proposes various mechanisms (sediment erosion/deposition, compaction, root decomposition/growth, soil swelling and folding of the root mat) for why marsh platform elevation

changes may occur, the precise mechanisms are never able to be fully constrained, as the surface elevation table apparatus groups processes into surface and below-ground surfaces. Specific mechanisms should, however, be tested on substrates in the laboratory, and this is often easier than directly observing the impact of storm surges in the field. These should be tested on both minerogenic and organic substrates. In so doing, we will be able to better understand the response of salt marsh substrates to loading during storm surges.

5.2.2 | Vertical recovery potential following unloading

The pre-consolidation pressure at Warton was higher than at Tillingham, implying that Warton sediments had previously been exposed to higher vertical effective stresses. The sediments were therefore lightly to heavily overconsolidated at Tillingham and heavily overconsolidated at Warton (OCR > 3; see Barnes, 2010), similar to the overconsolidation found by Brain et al. (2011) at Cowpen Marsh, UK. Such overconsolidation resulting from the high pre-consolidation pressure could occur due to vegetation removing moisture from the soil, alongside tidal exposure and a reduction in groundwater level, with the latter allowing desiccation and producing capillary suction stresses (Brain et al., 2011). The higher pre-consolidation pressures at Warton may reflect the coarser grain size and the higher marsh platform elevation within the tidal frame compared to Tillingham, which result in faster drainage and a longer duration and frequency of subaerial exposure, enhancing desiccation. During summer, neap tides rarely reach the marsh surface at Warton, allowing desiccation to occur, alongside a reduction in water table elevation (Barras & Paul, 2000). The combination of coarser grain size and a higher elevation within the tidal frame at Warton has thus enhanced desiccation and increased the pre-consolidation pressure and the OCR.

The pre-consolidation pressures at both Tillingham and Warton are unlikely to be reached by storm surges recorded near these sites. While substrate deformation in response to a storm surge is unlikely (as it would require full hydraulic disconnectivity at the marsh surface), any deformation would be fully recoverable if the applied vertical load did not exceed the pre-consolidation pressure. The high pre-consolidation stresses in the substrates tested here therefore imply that vertical total stresses applied by storm surges would not be able to produce irrecoverable compression. As such, the desiccation processes which originally generated the high pre-consolidation stresses may actually be increasing the substrate resistance to compression (a) by reducing the magnitude of compression experienced during a storm surge and (b) by ensuring that any axial displacement which does occur, is then recovered once the vertical total stress is no longer present.

Cahoon (2003) attributed marsh elevation changes following storm surge inundation to soil shrinkage (consolidation) at St. Marks River and Ochlockonee, Florida, and found that the original surface elevation was not recovered, with an overall reduction in surface elevation of 13–21 mm following the storm surge. This contrasts with deformation always being recoverable at Tillingham and Warton. Whether or not this difference in recoverability relates to the lower organic matter in UK marshes compared to US marshes remains to be seen. However, if consolidation can result in irrecoverable deformation, then understanding the conditions under which irrecoverable vertical displacement may occur is imperative to understand marsh vertical stability and improve marsh evolution models in the future.

Incomplete recovery will lower the marsh within the tidal frame and expose it to higher, more frequent, hydrostatic pressures from increased water depths. The increased flooding frequency may also increase sediment supply and near-surface accretion. There is therefore a need to understand the pre-consolidation pressure and OCR of salt marsh substrates, in order to understand the degree to which present marsh substrates are consolidated, how they may consolidate under future vertical loads, and whether they would remain consolidated after load removal. Understanding these three aspects of substrate characteristics and behaviour will allow for better near-future forecasts of marsh vertical stability.

It is clear from the results of this study that desiccation of Tillingham and Warton marsh substrates resulted in lower magnitudes of vertical displacement during loading than if desiccation had not taken place, and that this vertical displacement was also recoverable. Desiccation processes may thus increase marsh resistance to compression. The desiccation processes that generated the high pre-consolidation stresses will also have applied suction to the substrate, reducing the void ratio. As a reduced void ratio is linked to an increased substrate strength, desiccation processes may increase resistance to both compression and shear failure processes. Desiccation processes and the resultant suction stresses should therefore be included in marsh evolution models, due to both their influence on marsh substrate shear strength and also the resistance of the marsh to compression. By measuring suction and understanding the OCR and pre-consolidation pressure of a marsh substrate then feeding this data into models, autocompaction models could more accurately indicate both the magnitude of autocompaction and also whether the compression is recoverable through modification of the λ term, which accounts for compaction (see D'Alpaos et al., 2011; Goodwin & Mudd, 2019).

6 | CONCLUSIONS

Shear box and ring shear tests have allowed the analysis of salt marsh and tidal flat substrate response to the application of shear stress under laboratory-controlled drained conditions. The substrates tested here required continued shear stress application to produce deformation. These tests allowed separation of the cohesional and frictional components of shear strength and therefore provided an insight into possible controls on the shear strength of these substrates (particle size, the shape of the particle size distribution curve and void ratio). By comparing peak and residual shear strength, and the peak and residual friction angle, these tests allowed the separation of the influence of sediment and roots on marsh substrate shear strength.

The application of oedometer tests to salt marsh substrates has provided insight into both the magnitude of axial displacement and the recovery potential of marsh substrates following application of a vertical effective stress. Both the expected magnitude of displacement and recovery potential of a marsh substrate were affected by past stress conditions on the marsh (particularly due to desiccation). The high pre-consolidation stresses measured here highlight that, even under the worst possible conditions

(full hydraulic disconnectivity and rapid dissipation of pore water pressures), vertical total stresses applied by storm surges would not be able to produce irrecoverable displacement, as has been observed in some US marshes.

Future work is now needed to assess the heterogeneity in marsh substrate behaviour in response to applied shear stress across space. Furthermore, linking the shear box and ring shear data to tensile strength measurements of roots could provide evidence as to why the greatest reduction in strength between the peak and the residual scenarios is identified at the marsh surface. While this study assessed the impact of monotonic stresses on substrate shear strength, future work could look at cyclic application of shear stresses. This would more closely resemble the forces experienced in the field, mimicking the cyclic oscillations of pressure induced by changes in incident waves and tidal levels. Combining the drained shear box and ring shear tests with undrained strength measurements would also improve understanding of marsh substrate behaviour in response to applied stress, and thus marsh change over longer timescales, than the near-instantaneous timescale associated with *in-situ* undrained measurements.

While this research did not intend to mimic real-world processes, the understanding of soil geotechnical properties will allow improvement of models of marsh edge erosion processes in the future (e.g. Bendoni et al., 2014), ultimately improving our understanding of these processes and, therefore, marsh stability. Finally, the measurements reported in this paper will allow for future models of marsh geomorphological evolution to better represent these dynamic responses, along with their implications for the hydrological, sedimentological and ecological function of marsh systems.

ACKNOWLEDGEMENTS

This work was funded by the Natural Environment Research Council, UK (Grants No. NE/L002507/1, NE/R01082X/1 and NE/N015878/1) and the British Geological Survey (BGS). This paper is published with permission of the BGS Executive Director. The authors would also like to thank Sam Bithell, Simon Carr, Elizabeth Christie, Clementine Chirol, Ben Evans, Amy McGuire and James Pollard for help with fieldwork, and Peter Hobbs and Lee Jones for advice.

DATA AVAILABILITY STATEMENT

Datasets related to this paper will be accessible from PANGAEA data repository as soon as a the DOI is available.

ORCID

Helen Brooks https://orcid.org/0000-0002-8291-4070
Iris Moeller https://orcid.org/0000-0003-1971-2932
Tom Spencer https://orcid.org/0000-0003-2610-6201
Katherine Royse https://orcid.org/0000-0001-5660-2615

REFERENCES

Abernethy, B. & Rutherfurd, I.D. (2000) The effect of riparian tree roots on the mass-stability of riverbanks. *Earth Surface Processes and Landforms*, 25(9), 921–937. Available from: https://doi.org/10.1002/1096-9837(200008)25:9<921::AID-ESP93>3.0.CO;2-7

Alias, R., Kasa, A. & Taha, M.R. (2014) Particle size effect on shear strength of granular materials in direct shear test. *International Journal of Civil, Structural, Construction and Architectural Engineering*, 8(11), 733–736. Available from: https://doi.org/10.5281/zenodo.1096805

Allen, J.R.L. (1989) Evolution of salt-marsh cliffs in muddy and sandy systems: A qualitative comparison of British West-Coast estuaries. *Earth Surface Processes and Landforms*, 14(1), 85–92. Available from: https://doi.org/10.1002/esp.3290140108

Allen, J.R.L. (1999) Geological impacts on coastal wetland landscapes: Some general effects of sediment autocompaction in the Holocene of northwest Europe. *The Holocene*, 9(1), 1–12. Available from: https://doi.org/10.1191/095968399674929672

Allen, J.R.L. (2000) Morphodynamics of Holocene salt marshes: A review sketch from the Atlantic and Southern North Sea coasts of Europe. *Quaternary Science Reviews*, 19(12), 1155–1231. Available from: https://doi.org/10.1016/S0277-3791(99)00034-7

Baily, B. & Pearson, A.W. (2007) Change detection mapping and analysis of salt marsh areas of Central Southern England from Hurst Castle Spit to Pagham Harbour. *Journal of Coastal Research*, 23(6), 1549–1564. Available from: https://doi.org/10.2112/05-0597.1

Barnes, G. (2010) *Soil Mechanics: Principles and Practice*, 3rd edition. Basingstoke: Palgrave Macmillan.

Barras, B.F. & Paul, M.A. (2000) Post-reclamation changes in estuarine mudflat sediments at Bothkennar, Grangemouth, Scotland. In: Pye, K. & Allen, J.R.L. (Eds.) *Coastal and Estuarine Environments: Sedimentology, Geomorphology and Geoarchaeology*. London: The Geological Society of London, pp. 187–199.

Beaumont, N.J., Austen, M.C., Mangi, S.C. & Townsend, M. (2008) Economic valuation for the conservation of marine biodiversity. *Marine Pollution Bulletin*, 56(3), 386–396. Available from: https://doi.org/10.1016/j.marpolbul.2007.11.013

Bendoni, M., Francalanci, S., Cappietti, L. & Solari, L. (2014) On salt marshes retreat: Experiments and modeling toppling failures induced by wind waves. *Journal of Geophysical Research – Earth Surface*, 119(3), 603–620. Available from: https://doi.org/10.1002/2014JF003147

Bendoni, M., Mel, R., Solari, L., Lanzoni, S., Francalanci, S. & Oumeraci, H. (2016) Insights into lateral marsh retreat mechanism through localised field measurements. *Water Resources Research*, 52(2), 1446–1464. Available from: https://doi.org/10.1111/j.1752-1688.1969.tb04897.x

Bishop, A. & Henkel, D. (1962) *The Measurement of Soil Properties in the Triaxial Test*, 2nd edition. London: Arnold.

Blankespoor, B., Dasgupta, S. & Laplante, B. (2014) Sea-level rise and coastal wetlands. *Ambio*, 43(8), 996–1005. Available from: https://doi.org/10.1007/s13280-014-0500-4

Bolton, M.D. (1991) *A Guide to Soil Mechanics*, 3rd edition. London: Macmillan.

Brain, M.J., Kemp, A.C., Hawkes, A.D., Engelhart, S.E., Vane, C.H., Cahill, N., et al. (2017) Exploring mechanisms of compaction in salt-marsh sediments using Common Era relative sea-level reconstructions. *Quaternary Science Reviews*, 167, 96–111. Available from: https://doi.org/10.1016/j.quascirev.2017.04.027

Brain, M.J., Kemp, A.C., Horton, B.P., Culver, S.J., Parnell, A.C. & Cahill, N. (2015) Quantifying the contribution of sediment compaction to late Holocene salt-marsh sea-level reconstructions, North Carolina, USA. *Quaternary Research*, 83(1), 41–51. Available from: https://doi.org/10.1016/j.yqres.2014.08.003

Brain, M.J., Long, A.J., Petley, D.N., Horton, B.P. & Allison, R.J. (2011) Compression behaviour of minerogenic low energy intertidal sediments. *Sedimentary Geology*, 233(1–4), 28–41. Available from: https://doi.org/10.1016/j.sedgeo.2010.10.005

Brooks, H. (2020) *Salt marsh substrate composition and responses to applied stress*. PhD thesis, University of Cambridge.

Brooks, H., Möller, I., Carr, S., Chirol, C., Christie, E., Evans, B., et al. (2021) Resistance of salt marsh substrates to near-instantaneous hydrodynamic forcing. *Earth Surface Processes and Landforms*, 46(1), 67–88. Available from: https://doi.org/10.1002/esp.4912

BSI. (1990a) *BS1377 Part 7: Shear strength tests (total stress)*. London: British Standard Institution.

BSI. (1990b) *BS1377 Part 5: Compressibility, permeability and durability tests*. London: British Standard Institution.

BSI. (2015) *Code of Practise for Ground Investigations (new version). BS 5930*. London: British Standards Institution.

Cahoon, D.R. (2003) Storms as agents of wetland elevation change: Their impact on surface and subsurface sediment processes. In: *Proceedings of the International Conference on Coastal Sediments*. Corpus Christi, TX: World Scientific and East Meets West Productions, pp. 1–14.

Cahoon, D.R. (2006) A review of major storm impacts on coastal wetland elevations. *Estuaries and Coasts*, 29(6A), 889–898. Available from: https://doi.org/10.1007/BF02798648

Callaghan, D.P., Bouma, T.J., Klaassen, P., van der Wal, D., Stive, M.J.F. & Herman, R.M.J. (2010) Hydrodynamic forcing on salt-marsh development: Distinguishing the relative importance of waves and tidal flows. *Estuarine, Coastal and Shelf Science*, 89(1), 73–88. Available from: https://doi.org/10.1016/j.ecss.2010.05.013

Carr, S., Diggens, L. & Spencer, K. (2020) There's no such thing as "undisturbed" soil and sediment sampling: Sampler-induced deformation of salt-marsh sediments revealed by 3D x-ray computed tomography. *Journal of Soils and Sediments*, 20(7), 2960–2976. Available from: https://doi.org/10.1007/s11368-020-02655-7

Chen, Y., Thompson, C.E.L. & Collins, M.B. (2012) Saltmarsh creek bank stability: Biostabilisation and consolidation with depth. *Continental Shelf Research*, 35, 64–74. Available from: https://doi.org/10.1016/j.csr.2011.12.009

Chirol, C., Spencer, K.L., Carr, S.J., Moeller, I., Evans, B., Lynch, J., et al. (2021) Effect of vegetation cover and sediment type on 3D subsurface structure and shear strength in saltmarshes. *Earth Surface Processes and Landforms*, 46(11), 2279–2297. Available from: https://doi.org/10.1002/esp.5174

Cola, S., Sanavia, L., Simonini, P. & Schrefler, B.A. (2008) Coupled thermo-hydromechanical analysis of Venice lagoon salt marshes. *Water Resources Research*, 44(5), 1–16. Available from: https://doi.org/10.1029/2007WR006570

Crooks, S. & Pye, K. (2000) Sedimentological controls on the erosion and morphology of saltmarshes: Implications for flood defence and habitat recreation. In: Pye, K. & Allen, J.R.L. (Eds.) *Coastal and Estuarine Environments: Sedimentology, Geomorphology and Geoarchaeology*. London: The Geological Society of London, pp. 207–222.

Crooks, S., Schutten, J., Sheern, G.D., Pye, K. & Davy, A.J. (2002) Drainage and elevation as factors in the restoration of salt marsh in Britain. *Restoration Ecology*, 10(3), 591–602. Available from: https://doi.org/10.1046/j.1526-100X.2002.t01-1-02036

D'Alpaos, A., Mudd, S.M. & Carniello, L. (2011) Dynamic response of marshes to perturbations in suspended sediment concentrations and rates of relative sea level rise. *Journal of Geophysical Research – Earth Surface*, 116(4), 1–13. Available from: https://doi.org/10.1029/2011JF002093

DeLaune, R.D., Nyman, J.A. & Patrick, W.H., Jr. (1994) Peat collapse, ponding and wetland loss in a rapidly submerging coastal marsh. *Journal of Coastal Conservation*, 10(4), 1021–1030.

Docker, B.B. & Hubble, T.C.T. (2008) Quantifying root-reinforcement of river bank soils by four Australian tree species. *Geomorphology*, 11(3–4), 401–418. Available from: https://doi.org/10.1016/j.geomorph.2008.01.009

Elschot, K., Bouma, T.J., Temmerman, S. & Bakker, J.P. (2013) Effects of long-term grazing on sediment deposition and salt-marsh accretion rates. *Estuarine, Coastal and Shelf Science*, 133, 109–115. Available from: https://doi.org/10.1016/j.ecss.2013.08.021

Ford, H., Garbutt, A., Ladd, C., Malarkey, J. & Skov, M.W. (2016) Soil stabilization linked to plant diversity and environmental context in coastal wetlands. *Journal of Vegetation Science*, 27(2), 259–268. Available from: https://doi.org/10.1111/jvs.12367

Foster, N.M., Hudson, M.D., Bray, S. & Nicholls, R.J. (2013) Intertidal mudflat and saltmarsh conservation and sustainable use in the UK: A review. *Journal of Environmental Management*, 126, 96–104. Available from: https://doi.org/10.1016/j.jenvman.2013.04.015

Francalanci, S., Bendoni, M., Rinaldi, M. & Solari, L. (2013) Ecomorphodynamic evolution of salt marshes: Experimental observations of bank retreat processes. *Geomorphology*, 195, 53–65. Available from: https://doi.org/10.1016/j.geomorph.2013.04.026

French, J.R. (2006) Tidal marsh sedimentation and resilience to environmental change: Exploratory modelling of tidal, sea-level and sediment supply forcing in predominantly allochthonous systems. *Marine Geology*, 235(1–4), 119–136. Available from: https://doi.org/10.1016/j.margeo.2006.10.009

GDS Instruments Ltd. (2014) *Automatic Oedometer System (GDSAOS): Specification Datasheet*. http://www.gdsinstruments.com/gds-products/gds-automatic-oedometer-system

Giang, P.H.H., Van Lmpe, P.O., Van Lmpe, W.F., Menge, P., Cnudde, V. & Haegeman, W. (2017) Effects of particle characteristics on the shear strength of calcareous sand. *Acta Geotechnica Slovenica*, 14(2), 77–89.

Gibson, R.E. & Henkel, D.J. (1954) Influence of duration of tests at constant rate of strain on measured "drained" strength. *Geotechnique*, 4(1), 6–15. Available from: https://doi.org/10.1680/geot.1954.4.1.6

Godfrey, S., Cooper, J., Bezombes, F. & Plater, A. (2020) Monitoring coastal morphology: The potential of low-cost fixed array action cameras for 3D reconstruction. *Earth Surface Processes and Landforms*, 45(11), 2478–2494. Available from: https://doi.org/10.1002/esp.4892

Goodwin, G.C.H. & Mudd, S.M. (2019) High platform elevations highlight the role of storms and spring tides in salt marsh evolution. *Frontiers in Environmental Science*, 7, 1–14. Available from: https://doi.org/10.3389/fenvs.2019.00062

Gray, A.J. (1972) The ecology of Morecambe Bay. V. The salt marshes of Morecambe Bay. *Journal of Applied Ecology*, 9(1), 207–220. Available from: https://doi.org/10.2307/2402057

Hackney, C.T. & De La Cruz, A.A. (1980) *In situ* decomposition of roots and rhizomes of two tidal marsh plants. *Ecology*, 61(2), 226–231. Available from: https://doi.org/10.2307/1935178

Harmsworth, G.C. & Long, S.P. (1986) An assessment of saltmarsh erosion in Essex, England, with reference to the Dengie Peninsula. *Biological Conservation*, 35(4), 377–387. Available from: https://doi.org/10.1016/0006-3207(86)90095-9

Head, K. (1981) *Manual of Soil Laboratory Testing, Vol. 2: Permeability, Shear Strength and Compressibility Tests*. London: Pentech Press.

Head, K.H. (1994) *Manual of Soil Laboratory Testing, Vol. 2: Permeability, Shear Strength and Compressibility Tests*, 2nd edition. London: Pentech Press.

Hight, D.W., Paul, M.A., Barras, B.F., Powell, J.J.M., Nash, D.F.T., Smith, P.R., et al. (2003) The characterisation of the Bothkennar clay. In: *Proceedings of the International Workshop on Characterisation and Engineering Properties of Natural Soils*, Vol. 2. Boca Raton, FL: CRC Press, pp. 543–597.

Howes, B.L. & Teal, J.M. (1994) Oxygen loss from Spartina alterniflora and its relationship to salt marsh oxygen balance. *Oecologia*, 97(4), 431–438. Available from: https://doi.org/10.1007/BF00325879

Kara, E.M., Meghachou, M. & Aboubekr, N. (2013) Contribution of particle size ranges to sand friction. *Engineering, Technology & Applied Science Research*, 3(4), 497–501. Available from: https://doi.org/10.1039/F29837900755

Knappett, J.A. & Craig, R.F. (2012) *Craig's Soil Mechanics*, 8th edition. London/New York: Spoon Press/Taylor & Francis.

Kruskal, W.H. & Wallis, W.A. (1952) Use of ranks in one-criterion variance analysis. *Journal of the American Statistical Association*, 47(260), 583–621. Available from: https://doi.org/10.1080/01621459.1952.10483441

Lambert, R. (2000) Practical management of grazed saltmarshes. In: Sherwood, B.R., Gardiner, B.G. & Harris, T. (Eds.) *British Saltmarshes*. London: Forrest Text, pp. 333–340.

Latha, G.M. & Sitharam, T.G.G. (2008) Effect of particle size and gradation on the behaviour of granular materials simulated using DEM. *Indian Geotechnical Journal*, 38(1), 68–88.

Lehane, B.M. & Jardine, R.J. (1992) Residual strength characteristics of Bothkennar clay. *Géotechnique*, 42(2), 363–367. Available from: https://doi.org/10.1680/geot.1992.42.2.363

Leonardi, N., Ganju, N.K. & Fagherazzi, S. (2016) A linear relationship between wave power and erosion determines salt-marsh resilience to violent storms and hurricanes. *Proceedings of the National Academy of Sciences*, 113(1), 64–68. Available from: https://doi.org/10.1073/pnas.1510095112

Lo, V.B., Bouma, T.J., van Belzen, J., Van Colen, C. & Airoldi, L. (2017) Interactive effects of vegetation and sediment properties on erosion

of salt marshes in the Northern Adriatic Sea. *Marine Environmental Research*, 131, 32–42. Available from: https://doi.org/10.1016/j.marenvres.2017.09.006

Lupini, J.F., Skinner, A.E. & Vaughan, P.R. (1981) The drained residual strength of cohesive soils. *Geotechnique*, 31(2), 181–213. Available from: https://doi.org/10.1061/(ASCE)0733-9410(1994)120:5(856)

Mariotti, G. & Carr, J. (2014) Dual role of salt marsh retreat: Long-term loss and short-term resilience. *Water Resources Research*, 50(4), 2963–2974. Available from: https://doi.org/10.1002/2013WR014676

Mariotti, G. & Fagherazzi, S. (2010) A numerical model for the coupled long-term evolution of salt marshes and tidal flats. *Journal of Geophysical Research – Earth Surface*, 115(F1), 1–15. Available from: https://doi.org/10.1029/2009JF001326

Mason, D.C., Scott, T.R. & Dance, S.L. (2010) Remote sensing of intertidal morphological change in Morecambe Bay, U.K., between 1991 and 2007. *Estuarine, Coastal and Shelf Science*, 87(3), 487–496. Available from: https://doi.org/10.1016/j.ecss.2010.01.015

Möller, I. (2006) Quantifying saltmarsh vegetation and its effect on wave height dissipation: Results from a UK east coast saltmarsh. *Estuarine, Coastal and Shelf Science*, 69(3–4), 337–351. Available from: https://doi.org/10.1016/j.ecss.2006.05.003

Möller, I., Kudella, M., Rupprecht, F., Spencer, T., Paul, M., van Wesenbeeck, B.K., et al. (2014) Wave attenuation over coastal salt marshes under storm surge conditions. *Nature Geoscience*, 7(10), 727–731. Available from: https://doi.org/10.1038/ngeo2251

Möller, I. & Spencer, T. (2002) Wave dissipation over macro-tidal saltmarshes: Effects of marsh edge typology and vegetation change. *Journal of Coastal Research*, 36(36), 506–521. Available from: https://doi.org/10.2112/1551-5036-36.sp1.506

Mouazen, A.M. (2002) Mechanical behaviour of the upper layers of a sandy loam soil under shear loading. *Journal of Terramechanics*, 39(3), 115–126. Available from: https://doi.org/10.1016/S0022-4898(02)00008-3

Nyman, J.A., Delaune, R.D. & Patrick, W.H. (1990) Wetland soil formation in the rapidly subsiding Mississippi River Deltaic Plain: Mineral and organic matter relationships. *Estuarine, Coastal and Shelf Science*, 31(1), 57–69. Available from: https://doi.org/10.1016/0272-7714(90)90028-P

Ouyang, X., Lee, S.Y. & Connolly, R.M. (2017) The role of root decomposition in global mangrove and saltmarsh carbon budgets. *Earth-Science Reviews*, 166, 53–63. Available from: https://doi.org/10.1016/j.earscirev.2017.01.004

Pollen, N. & Simon, A. (2005) Estimating the mechanical effects of riparian vegetation on stream bank stability using a fiber bundle model. *Water Resources Research*, 41(7), 1–11. Available from: https://doi.org/10.1029/2004WR003801

Polvi, L.E., Wohl, E. & Merritt, D.M. (2014) Modeling the functional influence of vegetation type on streambank cohesion. *Earth Surface Processes and Landforms*, 39(9), 1245–1258. Available from: https://doi.org/10.1002/esp.3577

Pringle, A.W. (1995) Erosion of a cyclic saltmarsh in Morecambe Bay, North-West England. *Earth Surface Processes and Landforms*, 20(5), 387–405. Available from: https://doi.org/10.1002/esp.3290200502

Pye, K. & French, J. (1993) *Erosion and Accretion Processes on British Salt Marshes: Final Report to MAFF*. Cambridge: Cambridge Environmental Research Consultants.

Rupprecht, F., Möller, I., Evans, B., Spencer, T. & Jensen, K. (2015) Biophysical properties of salt marsh canopies – quantifying plant stem flexibility and above ground biomass. *Coastal Engineering*, 100, 48–57. Available from: https://doi.org/10.1016/j.coastaleng.2015.03.009

Schuerch, M., Spencer, T. & Evans, B. (2019) Coupling between tidal mudflats and salt marshes affects marsh morphology. *Marine Geology*, 412, 95–106. Available from: https://doi.org/10.1016/j.margeo.2019.03.008

Schuerch, M., Spencer, T., Temmerman, S., Kirwan, M.L., Wolff, C., Lincke, D., et al. (2018) Future response of global coastal wetlands to sea-level rise. *Nature*, 561(7722), 231–234. Available from: https://doi.org/10.1038/s41586-018-0476-5

Selig, E. & Roner, C. (1987) Effects of particle characteristics on behavior of granular material. *Transportation Research Record*, 1131, 1–6.

Simon, A. & Collison, A.J.C. (2002) Quantifying the mechanical and hydrologic effects of riparian vegetation on streambank stability. *Earth Surface Processes and Landforms*, 27(5), 527–546. Available from: https://doi.org/10.1002/esp.325

Simon A, Pollen N. (2006) A model of streambank stability incorporating hydraulic erosion and the effects of riparian vegetation. In *Proceedings of the 8th Federal Interagency Sedimentation Conference*, Reno, Nevada.

Spalding, M.D., McIvor, A.L., Beck, M.W., Koch, E.W., Möller, I., Reed, D.J., et al. (2014) Coastal ecosystems: A critical element of risk reduction. *Conservation Letters*, 7(3), 293–301. Available from: https://doi.org/10.1111/conl.12074

Spencer, T., Möller, I., Rupprecht, F., Bouma, T.J., van Wesenbeeck, B.K., Kudella, M., et al. (2015) Salt marsh surface survives true-to-scale simulated storm surges. *Earth Surface Processes and Landforms*, 41(4), 543–552. Available from: https://doi.org/10.1002/esp.3867

Strain, E.M.A., van Belzen, J., Comandini, P., Wong, J., Bouma, T.J. & Airoldi, L. (2017) The role of changing climate in driving the shift from perennial grasses to annual succulents in a Mediterranean saltmarsh. *Journal of Ecology*, 105(5), 1374–1385. Available from: https://doi.org/10.1111/1365-2745.12799

Tiwari, B. & Marui, H. (2005) A new method for the correlation of residual shear strength of the soil with mineralogical composition. *Journal of Geotechnical and Geoenvironmental Engineering*, 131(9), 1139–1150. Available from: https://doi.org/10.1061/(ASCE)1090-0241(2005)131:9(1139)

Tonelli, M., Fagherazzi, S. & Petti, M. (2010) Modeling wave impact on salt marsh boundaries. *Journal of Geophysical Research, Oceans*, 115(C9), 1–17. Available from: https://doi.org/10.1029/2009JC006026

Van der Wal, D. & Pye, K. (2004) Patterns, rates and possible causes of saltmarsh erosion in the Greater Thames area (UK). *Geomorphology*, 61(3–4), 373–391. Available from: https://doi.org/10.1016/j.geomorph.2004.02.005

Van Eerdt, M.M. (1985a) Salt marsh cliff stability in the Oosterschelde. *Earth Surface Processes and Landforms*, 10(2), 95–106. Available from: https://doi.org/10.1002/esp.3290100203

Van Eerdt, M.M. (1985b) The influence of vegetation on erosion and accretion in salt marshes of the Oosterschelde, The Netherlands. *Vegetatio*, 62(1–3), 367–373. Available from: https://doi.org/10.1007/BF00044763

Vangla, P. & Latha, G.M. (2015) Influence of particle size on the friction and interfacial shear strength of sands of similar morphology. *International Journal of Geosynthetics and Ground Engineering*, 1(1), 1–12. Available from: https://doi.org/10.1007/s40891-014-0008-9

Wang, H., van der Wal, D., Li, X., van Belzen, J., Herman, P.M.J., Hu, Z., et al. (2017) Zooming in and out: Scale dependence of extrinsic and intrinsic factors affecting salt marsh erosion. *Journal of Geophysical Research – Earth Surface*, 122(7), 1455–1470. Available from: https://doi.org/10.1002/2016JF004193

Watts, C.W., Tolhurst, T.J., Black, K.S. & Whitmore, A.P. (2003) *In situ* measurements of erosion shear stress and geotechnical shear strength of the intertidal sediments of the experimental managed realignment scheme at Tollesbury, Essex, UK. *Estuarine, Coastal and Shelf Science*, 58(3), 611–620. Available from: https://doi.org/10.1016/S0272-7714(03)00139-2

Zhang, H. & Hartge, K. (1990) Cohesion in unsaturated sandy soils and the influence of organic matter. *Soil Technology*, 3(4), 311–326. Available from: https://doi.org/10.1016/0933-3630(90)90013-S

How to cite this article: Brooks, H., Moeller, I., Spencer, T., Royse, K., Price, S. & Kirkham, M. (2022) How strong are salt marshes? Geotechnical properties of coastal wetland soils. *Earth Surface Processes and Landforms*, 1–19. Available from: https://doi.org/10.1002/esp.5322